Check for updates

Singh Pooja (Orcid ID: 0000-0001-6576-400X)

Peichel Catherine L. (Orcid ID: 0000-0002-7731-8944)

Genomic basis of Y-linked dwarfism in cichlids pursuing alternative reproductive tactics

Pooja Singh[1,2,3], Michael Taborsky[4,5,6], Catherine L. Peichel[7], and Christian Sturmbauer[1]

[1]Institute of Biology, University of Graz, A-8010 Graz, Austria

[2]Aquatic Ecology Division, Institute of Ecology and Evolution, University of Bern, CH-3012 Bern, Switzerland

[3]Swiss Federal Institute of Aquatic Science and Technology (EAWAG), CH-6047 Kastanienbaum, Switzerland

[4]Behavioural Ecology Division, Institute of Ecology and Evolution, University of Bern, CH-3032 Hinterkappelen, Switzerland

[5]Max Planck Institute of Animal Behavior, D-78467 Konstanz, Germany

[6]Institute for Advanced Study (Wissenschaftskolleg) Berlin, D-14193 Berlin, Germany

[7]Evolutionary Ecology Division, Institute of Ecology and Evolution, University of Bern, CH-3012 Bern, Switzerland

Corresponding author: Pooja Singh (pooja.singh09@gmail.com)

Accepted Article

source: https://doi.org/10.48350/176756 | downloaded: 25.4.2024

Abstract

Sexually antagonistic selection, which favours different optimums in males and females, is predicted to play an important role in the evolution of sex chromosomes. Body size is a sexually antagonistic trait in the shell-brooding cichlid fish *Lamprologous callipterus* as

This article has been accepted for publication and undergone full peer review but has not been through the copyediting, typesetting, pagination and proofreading process which may lead to differences between this version and the Version of Record. Please cite this article as doi: 10.1111/mec.16839

This article is protected by copyright. All rights reserved.

1365294x, ja, Downloaded from https://onlinelibrary.wiley.com/doi/10.1111/mec.16839 by Universität Bern, Wiley Online Library on [10/01/2023]. See the Terms and Conditions (https://onlinelibrary.wiley.com/terms-and-conditions) on Wiley Online Library for rules of use; OA articles are governed by the applicable Creative Commons License

'bourgeois' males must be large enough to carry empty snail shells to build nests whereas females must be small enough to fit into shells for breeding. In this species, there is also a second male morph: smaller 'dwarf' males employ an alternative reproductive strategy by wriggling past spawning females into shells to fertilise eggs. *L. callipterus* male morphology is passed strictly from father to son, suggesting Y-linkage. However, sex chromosomes had not been previously identified in this species, and the genomic basis of size dimorphism was unknown. Here we used whole-genome sequencing to identify a 2.4 Mb sex-linked region on scaffold_23 with reduced coverage and SNP density in both male morphs compared to females. Within this sex region, distinct Y-haplotypes delineate the two male morphs, and candidate genes for body size (GHRHR, a known dwarfism gene) and sex determination (ADCYAP1R1) are in high linkage disequilibrium (LD). Because differences in body size between females and males are under strong selection in *L. callipterus*, we hypothesise that sexual antagonism over body size initiated early events in sex chromosome evolution, followed by Y divergence to give rise to bourgeois and dwarf male reproductive strategies. Our results are consistent with the hypothesis that sexually antagonistic traits should be linked to young sex chromosomes.

Keywords: sexual conflict, sex chromosome evolution, alternative reproductive tactics, supergenes, dwarfism, growth

Introduction

Sex determination is extremely diverse across eukaryotes and can be controlled environmentally or genetically (D. Bachtrog et al., 2014). In most organisms with genetic control, the sex-determining locus is carried on a sex chromosome. Highly differentiated (i.e. heteromorphic) sex chromosome pairs, such as the XY chromosome pair in mammals and ZW chromosome pair in birds, have repeatedly evolved across the tree of life (D. Bachtrog

Accepted Article

1365294x, ja, Downloaded from https://onlinelibrary.wiley.com/doi/10.1111/mec.16839 by Universität Bern, Wiley Online Library on [10/01/2023]. See the Terms and Conditions (https://onlinelibrary.wiley.com/terms-and-conditions) on Wiley Online Library for rules of use; OA articles are governed by the applicable Creative Commons License

et al., 2014). The first step in the evolution of sex chromosomes from autosomes in species with separate sexes is believed to be the acquisition of a sex-determining gene on the Y or W chromosome (B. Charlesworth & Charlesworth, 2000; Brian Charlesworth, 1996). When this is followed by recombination suppression between the new sex chromosome pair, possibly via an inversion, degeneration of the Y or W chromosome occurs, leading to heteromorphic sex chromosome pairs (Doris Bachtrog, 2013; D. Charlesworth, Charlesworth, & Marais, 2005).

Several models to explain the repeated loss of recombination on sex chromosomes have been proposed (reviewed by Ponnikas et al. 2018). The prevailing model stipulates that sexually antagonistic selection can drive recombination suppression because it favours linkage between the sex-determining gene and a locus with sexually antagonistic effects (i.e. beneficial in one sex and detrimental in the other) (D. Charlesworth & Charlesworth, 1980; Rice, 1987). However, the broad applicability of the sexual antagonism hypothesis of sex chromosome evolution is still debated as it has been challenging to demonstrate empirically (Ironside, 2010; Ponnikas et al., 2018). One challenge is that in old and/or heteromorphic sex chromosome systems, it is difficult to disentangle whether recombination suppression was initiated due to the presence of sexually antagonistic loci or whether sexually antagonistic loci accumulated after recombination was suppressed. Younger and/or less differentiated (i.e. homomorphic) sex chromosomes are more promising systems to test whether sexually antagonistic selection has played a role in the evolution of sex chromosomes (Doris Bachtrog, 2013; Ponnikas et al., 2018). Indeed, sexually antagonistic traits are linked to young sex chromosomes in guppies (Almeida et al., 2020; Sandkam et al., 2021; Wright et al., 2017), stickleback (Kitano et al., 2009), and cichlids (R. B. Roberts, Ser, & Kocher, 2009). These studies highlight the value of studying traits that are known to be sexually antagonistic and then determining whether they are associated with young sex chromosome systems.

Accepted Article

1365294x, ja, Downloaded from https://onlinelibrary.wiley.com/doi/10.1111/mec.16839 by Universität Bern, Wiley Online Library on [10/01/2023]. See the Terms and Conditions (https://onlinelibrary.wiley.com/terms-and-conditions) on Wiley Online Library for rules of use; OA articles are governed by the applicable Creative Commons License

Accepted Article

Adaptive radiations of cichlid fish harbour hundreds of recently diverged species that have young and homomorphic sex chromosomes (Ozouf-Costaz et al., 2017; Poletto et al., 2010), with a high turnover of sex determination mechanisms even among closely related species (El Taher et al., 2021; Gammerdinger & Kocher, 2018). We hypothesise that sexually antagonistic selection may play an important role in sex chromosome evolution in cichlid fishes, as many sexually dimorphic traits related to body colour, body size, and behaviour are found in this lineage (Lande, Seehausen, & Van Alphen, 2001; M. Taborsky, 2001). Indeed, in several sexually dimorphic cichlid species from Lake Malawi, the sexually antagonistic 'orange blotch' body colour patterning is associated with the evolution of a novel sex determination locus (Roberts et al. 2009). Furthermore, as cichlid sex chromosomes are young and homomorphic, studies will not be confounded by the effects of recombination suppression that happened a long time in the past. Thus, cichlids are an excellent system to investigate the sexual antagonism theory of sex chromosome evolution.

Here, we focused on the cichlid *Lamprologous callipterus* from Lake Tanganyika in East Africa (Figure 1A) that exhibits the most extreme sexual size dimorphism so far known among animals in which males exceed females in size. Nest-building "bourgeois" males have a 12-fold difference in body mass compared to females (Schütz & Taborsky 2000; see Taborsky 1997 for terminology). These males must exceed a minimum size threshold in order to carry empty gastropod shells to build a nest, and females must be small enough to fit into these shells for spawning and brood care (D. Schütz, Parker, Taborsky, & Sato, 2006; D. Schütz & Taborsky, 2005). Consequently, body-size is a sexually antagonistic trait in this species due to differential fitness effects of body-size for shell-brooders. In addition to the bourgeois males, so-called "dwarf males" that average only 2.4% of the mass of bourgeois males also exist in this species (Figure 1A). These males compete with bourgeois nest owners for egg fertilisation by applying an alternative reproductive strategy that involves wriggling past spawning females into the shell to fertilise eggs from this advantageous position (Figure 1A) (Wirtz-Ocana, Meidl, Bonfils, & Taborsky, 2014). Thus, dwarf males

13652294x, ja, Downloaded from https://onlinelibrary.wiley.com/doi/10.1111/mec.16839 by Universität Bern, Wiley Online Library on [10/01/2023]. See the Terms and Conditions (https://onlinelibrary.wiley.com/terms-and-conditions) on Wiley Online Library for rules of use; OA articles are governed by the applicable Creative Commons License

need to be even smaller than females (Tetsu Sato, Hirose, Taborsky, & Kimura, 2004). Bourgeois males acquire more mates than dwarf males, but dwarf males are more successful during direct sperm competition in laboratory trials (Dolores Schütz, Pachler, Ripmeester, Goffinet, & Taborsky, 2010; Michael Taborsky, Schütz, Goffinet, & Doorn, 2018; Wirtz-Ocana et al., 2014). Dwarf males are much rarer than bourgeois males in natural populations (von Kuerthy & Taborsky, 2016; Wirtz-Ocana et al., 2014). Negative frequency dependent selection is thought to be responsible for the relative numbers of dwarf and bourgeois males in nature, as these tactics are fixed for life and hence should yield similar fitness returns (Brockmann, H.J. & Taborsky, 2008; Parker, 1984; M Taborsky & Brockmann, 2010).

Experimental pedigrees have shown that reproductive tactic and body size in *L. callipterus* males adhered to the expectation of a Y-linked Mendelian trait controlled by a single locus (Wirtz-Ocana et al., 2014). Bourgeois males only sire bourgeois sons and dwarf males only sire dwarf sons, while daughters do not differ in any respect between these two types of males (Wirtz-Ocana et al., 2014). These results suggest that Y-linkage has resolved sexual antagonism over body size between males and females. However, neither the sex chromosomes nor the genes controlling male body size have yet been identified in this species. It is also unclear which of the two male types is the ancestral state.

In this study, we investigate the genomic basis of male body size in *L. callipterus* using whole-genome resequencing data from dwarf and bourgeois males, and their daughters (Table 1). Dwarf males initially grow at a faster rate than bourgeois males, but growth halts early in ontogeny (Wirtz-Ocana, Schütz, Pachler, & Taborsky, 2013), and bourgeois males continue to grow indefinitely (M. Taborsky, 2001) (Figure 1B). Thus, we hypothesised that the dwarf determining gene may encode a growth factor. We tested whether such a factor was linked to the sex-determining region, as the sexual antagonism hypothesis outlined above would predict. To investigate this hypothesis, we first needed to characterise the sex-

Accepted Article

1365294x, ja, Downloaded from https://onlinelibrary.wiley.com/doi/10.1111/mec.16839 by Universität Bern, Wiley Online Library on [10/01/2023]. See the Terms and Conditions (https://onlinelibrary.wiley.com/terms-and-conditions) on Wiley Online Library for rules of use; OA articles are governed by the applicable Creative Commons License

determining region. The karyotype of *L. callipterus* has not been studied, but karyotypes of other Lamprologini and related cichlids show no sex chromosome differentiation (Ozouf-Costaz et al., 2017). However, genomic data provide higher resolution into the subtle molecular differences between sexes in species with homomorphic sex chromosomes (Fontaine et al., 2017; Gammerdinger & Kocher, 2018). We compared whole genomes of males and females to identify regions of differentiation between the sexes and the morphs. In addition to *L. callipterus* samples, we included males and females of six related species from the Lamprologini tribe (see Table 1) for a comparative phylogenomic perspective on sex-determination and body-size evolution.

Materials and Methods

Sampling and sequencing

Sampling was conducted at the breeding facility at the Ethologische Station Hasli, University of Bern, Switzerland. Genomic DNA was extracted from fin clips of males and females of five species and males only of two species for which females were not available (Table 1). The stock population of the target species *L. callipterus* originated from the southern end of Lake Tanganyika near Mpulungu. Two *L. callipterus* dwarf males and two bourgeois males, as well as one daughter per male were sampled (See File S1 for genetic and biological relatedness) because it is easier to identify sex chromosomes in related individuals (Palmer et al. 2019). The TrueSeq DNA Library Preparation Kit was used for library preparation, and samples were sequenced at the Vienna BioCentre Sequencing Facility in Austria. The libraries were sequenced on eight lanes of an Illumina HiSeq 2500 machine generating ~125 million paired end reads (120 bp in length) per sample.

Accepted Article

1365294x, ja, Downloaded from https://onlinelibrary.wiley.com/doi/10.1111/mec.16839 by Universität Bern, Wiley Online Library on [10/01/2023]. See the Terms and Conditions (https://onlinelibrary.wiley.com/terms-and-conditions) on Wiley Online Library for rules of use; OA articles are governed by the applicable Creative Commons License

Reference-based assembly and characterisation of sex-determining region coverage

Raw Illumina reads were trimmed using fastx-trimmer (http://hannonlab.cshl.edu/fastx_toolkit v0.13). Reads were mapped to the *Neolamprologous brichardi* genome (Brawand et al., 2014), which was chosen because it is from the most closely-related cichlid species to our focal species (Darolti & Mank, 2022). However, to verify our results, we also mapped our data to the high-quality genome of *Oreochromis niloticus* (Conte, Gammerdinger, Bartie, Penman, & Kocher, 2017). See Results and Figures S2 – S4 for details. While *N. brichardi* is the most closely related reference genome, it is not the best assembled reference cichlid genome and there are trade-offs that must be considered when picking the best reference genome for sex chromosome mapping. As we are attempting to identify a young and homomorphic sex chromosome, we chose to use a more closely related reference. Read mapping was conducted using bowtie2 v2.2.7 (Langmead, Trapnell, Pop, & Salzberg, 2009) in the "very-sensitive" mode with no mixed alignments and retaining only concordantly mapped reads. We obtained an average coverage of ~25X across the genome (Table S1). Coverage of windows across the genome was calculated using bedtools v2.17 (Quinlan & Hall, 2010). The genome-wide coverage analysis was performed using 1 Mb moving windows with a 0.5 Mb step-size for all scaffolds with more than three windows. The scaffold_23 and scaffold_36 coverage analysis was performed using 30 kb moving windows with a 15 kb step-size. For each window, coverage was defined as the total number of times each site was sequenced divided by the number of sites that were sequenced. The data were normalized by dividing the coverage per window with average coverage per sample. To identify candidate sex chromosomes, the following calculation was used: $\log_2$(average male coverage / average female coverage). Negative values would indicate reduced coverage in males, i.e. a differentiated Y region. To identify regions of differentiation between bourgeois and dwarf males the following calculation was used: $\log_2$(average dwarf male coverage / average bourgeois male coverage). Regions in the genome with

Accepted Article

1365294x, ja, Downloaded from https://onlinelibrary.wiley.com/doi/10.1111/mec.16839 by Universität Bern, Wiley Online Library on [10/01/2023]. See the Terms and Conditions (https://onlinelibrary.wiley.com/terms-and-conditions) on Wiley Online Library for rules of use; OA articles are governed by the applicable Creative Commons License

Accepted Article

significantly reduced coverage (i.e. outliers) were defined as windows in the bottom 1% of the male:female coverage distribution. A permutation test using 20,000 permutations implemented in R (v4.0.2) was used to calculate if the coverage on scaffold_23 and scaffold_36 was significantly lower than the other scaffolds (i.e. autosomes). The permutation test was repeated after dividing scaffold_23 into two regions that represented the two peaks identified in the coverage density plots shown in Figure 1D, F: (1) the region from 1bp to 2.4 Mb and (2) the region from 2.4 Mb – 6.8 Mb. The permutation test was also repeated after dividing scaffold_36 into two regions that represented the two peaks identified in the coverage density plots shown in Figure 1D: (1) the region from 2.0 – 3.5 Mb and (2) the region from 1.0 Mb – 2.0 Mb and 3.5 Mb – 4.9 Mb.

SNP calling, F_{ST}, LD and inversion analysis

SAMtools v1.3 and bcftools v1.10.2 (Li et al., 2009) were used for calling and genotyping SNPs across all *L. callipterus* samples against the *N. brichardi* reference genome with default settings. SNPs passing the following filters were retained: sample and site DP ≥ 5, genotype quality ≥ 30, mapping quality ≥ 30, and missingness < 0.25. VCFtools v0.1.13 was used to calculate SNP density in dwarf males, bourgeois males and females. SNP density was normalised by the genome-wide average SNP density per sample. Permutation tests with 20,000 permutations implemented in R v4.0.2 were used to calculate if SNP density on scaffold_23 and scaffold_36 was significantly different from the rest of the genome. F_{ST} was calculated using PopGenome R package (Pfeifer, Wittelsbürger, Ramos-Onsins, & Lercher, 2014) in nonoverlapping windows of 30 kb. Significant differences in F_{ST} were estimated using the Wilcoxon rank sum test implemented in R v4.0.2. Outliers were defined as having greater values than the genome-wide 95th percentile or lower values than the genome-wide 5th percentile, depending on the analysis conducted. Sample relatedness was calculated using VCFtools v0.1.13 –relatedness2 option (File S1). Linkage disequilibrium (LD) across

13652294x, ja, Downloaded from https://onlinelibrary.wiley.com/doi/10.1111/mec.16839 by Universität Bern, Wiley Online Library on [10/01/2023]. See the Terms and Conditions (https://onlinelibrary.wiley.com/terms-and-conditions) on Wiley Online Library for rules of use; OA articles are governed by the applicable Creative Commons License

all *L. callipterus* samples was calculated as r^2 using the gpart package in R v4.0.2 with a MAF filter of < 0.05. LD heatmaps were plotted using the gpart LDBlockHeatmap function (Kim et al., 2019). Inversion analysis was conducted using two independent tools: LUMPY v2.13 (Layer, Chiang, Quinlan, & Hall, 2014) and DELLY v0.7.2 (Rausch et al., 2012) with default settings on the mapped BAM files for all *L. callipterus* samples.

Phylogenomics

We applied a gene tree vs species tree approach to investigate the evolution of sex chromosomes in the lamprologini clade. A tailored FASTA genome file was built for each individual using ANGSD v0.930 -dofasta function (Korneliussen, Albrechtsen, & Nielsen, 2014), which assembles FASTA-format genome sequences by picking the most common base per position in the mapped reads for each individual. Gene sequences for every second gene in the reference genome were extracted using bedtools v2.17 (Quinlan & Hall, 2010) and aligned using MAFFT v7.273 (Yamada, Tomii, & Katoh, 2016). Using every second gene provided a genome-wide overview with reduced computation time. Individual gene trees were constructed using the RAxML v8.2.9 (Stamatakis, 2014) GTRCAT method with 100 bootstrap replicates. A genome phylogeny was estimated using a coalescent approach using ASTRAL-II (Mirarab & Warnow, 2015) with the 11,855 gene trees and *N. brichardi* as the outgroup. Alignments of genes in the most diverged sex-region of scaffold_23 from 1.18 – 1.28 Mb were built as outlined above but with 1000 bootstrap replicates.

Signatures of selection

As body-size is an important trait across the whole Lamprologini clade, we tested for signatures of selection on the candidate dwarfism gene *GHRHR*. Exon sequences of the

Accepted Article

1365294x, ja, Downloaded from https://onlinelibrary.wiley.com/doi/10.1111/mec.16839 by Universität Bern, Wiley Online Library on [10/01/2023]. See the Terms and Conditions (https://onlinelibrary.wiley.com/terms-and-conditions) on Wiley Online Library for rules of use; OA articles are governed by the applicable Creative Commons License

gene were extracted from the reconstructed fasta genomes generated for the phylogenies using bedtools v2.17 (Quinlan & Hall, 2010). The exons were concatenated, and aligned using MAFFT v7.273 (Yamada et al., 2016). End stop codons were removed, and pairwise dN/dS was calculated using random models in PAML (Yang, 2007).

Results

Identification of sex-linked scaffolds in *L. callipterus*

To identify the sex-determining region in *L. callipterus*, we analysed the genomic coverage of mapped reads from eight individuals (two bourgeois males, two dwarf males and four females; Table 1) to the reference congener *N. brichardi* (female) genome (Brawand et al., 2014). Approximately 80% of the ~120 million paired end reads per sample mapped to the reference genome with average genome-wide coverage of 20X – 30X across samples (Table S1). We compared normalised genomic coverage between males and females to identify regions of reduced coverage in males, as diverged Y reads will no longer map to the X chromosome. Coverage analysis using a 1.0 Mb moving window and 0.5 Mb step-size revealed a small region on scaffold_23 with significantly reduced coverage outlier windows (below the bottom 1% of the genome-wide average), compared to the rest of the genome, in the two bourgeois males vs the four females (Figure 1C), as well as in the two dwarf males vs the four females (Figure 1E). Another small region of reduced coverage was identified on scaffold_36 in the two bourgeois males vs the four females (Figure 1C). The coverage in the outlier windows on scaffold_36 was the most extreme outlier across the genome of the bourgeois males (Figure 1D, permutation test $p = 0$). The coverage in the outlier windows on scaffold_23 was the second most extreme outlier across the genome of bourgeois males (Figure 1D, permutation test $p < 5.0e^{-5}$) and the most extreme outlier in the dwarf males (Figure 1F, permutation test $p = 0$). A comparison of coverage between dwarf and bourgeois

Accepted Article

1365294x, ja, Downloaded from https://onlinelibrary.wiley.com/doi/10.1111/mec.16839 by Universität Bern, Wiley Online Library on [10/01/2023]. See the Terms and Conditions (https://onlinelibrary.wiley.com/terms-and-conditions) on Wiley Online Library for rules of use; OA articles are governed by the applicable Creative Commons License

males suggested that the small region on scaffold_23 had lower coverage in the dwarf males compared to the bourgeois males, but it was not significant (Grubbs's outlier test p = 0.431; Figure S1). The density profile of $\log_2$ M:F coverage of all windows on scaffold_36 was bimodal for bourgeois males: the right peak contained windows from 1.0 bp – 2Mbp and 3.5 – 4.9 Mb with coverage similar to autosomal scaffolds, and the left peak contained windows from 2.0 – 3.5 Mb with lower coverage (Figure 1D). The density profile of $\log_2$ M:F coverage of all windows on scaffold_23 was bimodal for both male morphs (Figure 1D,F). The left peak contained windows from 1.0 bp – 2.4 Mb with lower $\log_2$ M:F coverage, and the right peak contained windows from 2.4 – 6.8 Mb with coverage similar to autosomal scaffolds. Thus, the region from 1.0 bp – 2.4 Mb on scaffold_23, which is shared by both male morphs, is hereon considered the putative sex-linked region in *L. callipterus*. The region from 2.0 – 3.5 Mb on scaffold_36 is a candidate sex-linked region specific to the bourgeois males.

Combining genomic coverage and SNP density can be useful for characterising sex-linked regions (Palmer, Rogers, Dean, & Wright, 2019; Wright et al., 2017). In regions where there is some differentiation (i.e. sequence divergence) between the X and the Y but not yet degeneration to the point where sequence reads from the Y chromosome no longer map to the reference genome, there will be more SNPs in males than in females. However, if the Y has degenerated, SNP density will be lower in males. We identified 9,135,392 SNPs across the genome of the *L. callipterus* males and females, of which 97,746 SNPs were on scaffold_23. For the coverage and SNP density analysis, we divided the 1Mb windows on scaffold_23 into two subsets based on the two coverage peaks (Figure 1D,F): (1) the region from 1.0 bp to 2.4 Mb; and (2) the region from 2.4 to 6.8 Mb. We found that windows from the 1.0 bp to 2.4 Mb region had significantly lower bourgeois M:F coverage relative to the rest of the genome (permutation test $p < 5.0e^{-5}$) but no significant increase in bourgeois M:F SNP density (permutation test $p = 0.15$) (Figure 2A). The region from 1.0 bp to 2.4 Mb had significantly lower dwarf M:F coverage (permutation test $p = 0$) and also significantly higher

Accepted Article

1365294x, ja, Downloaded from https://onlinelibrary.wiley.com/doi/10.1111/mec.16839 by Universität Bern, Wiley Online Library on [10/01/2023]. See the Terms and Conditions (https://onlinelibrary.wiley.com/terms-and-conditions) on Wiley Online Library for rules of use; OA articles are governed by the applicable Creative Commons License

Accepted Article

dwarf M:F SNP density (permutation test $p < 0.03$) relative to the rest of the genome (Figure 2B). The windows from the 2.4 - 6.8 Mb region did not have significantly lower M:F coverage compared to the rest of the genome (permutation test $p > 0.05$). However, this region had significantly elevated M:F SNP density in the dwarf males (permutation test $p = 4.5e^{-4}$) but not in the bourgeois males (permutation test $p = 0.76$). For the bourgeois male specific candidate region from 2.0 – 3.5 Mb on scaffold_36, the M:F coverage was significantly reduced (permutation test $p = 0$), but there was no increase but rather a decrease in M:F SNP density compared to the rest of the genome. When we repeated these analyses with the *O. niloticus* reference genome (NB: *N. brichardi* scaffold_23 corresponds to *O. niloticus* LG18:19.3 – 26.1 Mbp, see Figure S2) we discovered that the *N. brichardi* sex region on scaffold_23 may represent a subset of a putatively larger sex region on LG18 (Figure S3, S4). However, the genome-wide coverage results were noisier with many coverage outliers (Figure S5). This is not surprising given the large divergence times (~24 MYA, Irisarri, Singh et al. 2018) between *O. niloticus* and *L. callipterus*, but also because the sex region in *L. callipterus* is young and not strongly differentiated. *O. niloticus* LG18:19.3 – 26.1 Mbp was a significant outlier in the dwarf males:females comparison (Figure S5).

Refining patterns of sex linkage and candidate genes on scaffold_36

To further examine the pattern of divergence across scaffold_36 in *L. callipterus* bourgeois males versus females, we calculated SNP density and F_{ST} using 30 kb windows (Figure S6). There was a decrease in M:F SNP density beyond the 5th percentile of genome-wide SNP density at 2.0 – 2.4 Mbp and 3.6 – 3.9 Mbp (Figure S6A). There was however no clear increase in F_{ST} beyond the genome-wide 95th percentile across scaffold_36 (Figure S6B). Of the 28 genes annotated in the region of reduced coverage on scaffold_36, none had a function that could putatively be associated with a phenotype that delineates the bourgeois male reproductive tactic (File S2). However, one gene in this region, *endothelin-2* (EDN2) is associated with ovary development in mice (Ko et al., 2006). Because this region only had

1365294x, ja, Downloaded from https://onlinelibrary.wiley.com/doi/10.1111/mec.16839 by Universität Bern, Wiley Online Library on [10/01/2023]. See the Terms and Conditions (https://onlinelibrary.wiley.com/terms-and-conditions) on Wiley Online Library for rules of use; OA articles are governed by the applicable Creative Commons License

reduced coverage in bourgeois males vs females and did not have strong evidence of genes with sex-associated phenotypes, the region of reduced coverage on scaffold_23 was the best candidate for the *L. callipterus* sex region, and we therefore concentrated our further analyses on this scaffold.

Refining patterns of sex linkage on scaffold_23

To further examine the spatial pattern of divergence across scaffold_23 in *L. callipterus* bourgeois and dwarf males versus females, we calculated M:F coverage, SNP density, and F_{ST} in 30 kb windows (Figure 3). The most extreme coverage reduction in both males was between 1.18 Mb and 1.28 Mb, which represented the lowest 0.001% of the genome-wide M:F coverage (Figure 3A, B). This decrease in coverage was recapitulated when both male morphs were collectively compared to the females (Figure S7A). The reduction in coverage in dwarf males vs females ($\log_2$ M:F = -0.6) was two-fold lower than that of bourgeois males vs. females ($\log_2$ M:F = -0.3) within the 1.18 – 1.28 Mb region, such that the dwarf males had reduced coverage when compared to bourgeois males ($\log_2$ dwarf males:bourgeois males = -0.3; Figure S7B). This suggests that the sex region on scaffold_23 is distinct between the dwarf and bourgeois males.

When SNP density was analysed together for all windows within the two regions of scaffold_23, there was either an increase in M:F SNP density (consistent with differentiation between the X and the Y) or no change in M:F SNP density compared to the rest of the genome (Figure 2). However, when the smaller 30kb windows were analysed individually, windows with a decrease in M:F SNP density (consistent with degeneration of the Y) beyond the 5th percentile of genome-wide SNP density can also be seen around 2.0 Mb and 6.2 Mb in the bourgeois M:F comparison (Figure 3C) and around 1.2 Mb, 2.0 Mb, 3.9 Mb and 6.2 Mb in the dwarf M:F comparison (Figure 3D).

Accepted Article

1365294x, ja, Downloaded from https://onlinelibrary.wiley.com/doi/10.1111/mec.16839 by Universität Bern, Wiley Online Library on [10/01/2023]. See the Terms and Conditions (https://onlinelibrary.wiley.com/terms-and-conditions) on Wiley Online Library for rules of use; OA articles are governed by the applicable Creative Commons License

Accepted Article

Male-Female F_{ST} quantifies differences in allele frequency between the sexes, and thus can be used to detect differentiation in very young sex chromosomes (Gammerdinger, Conte, Acquah, Roberts, & Kocher, 2014; Vicoso, 2019). F_{ST} will identify regions where males are heterozygous and females are homozygous, consistent with expectations for a sex-linked region. We analysed F_{ST} between *L. callipterus* males and females and found significantly higher F_{ST} from 1 bp to 2.4 Mb of scaffold_23 compared to the remainder of scaffold_23 (Wilcoxon rank sum test $p < 2.2e\text{-}^{16}$) between dwarf males versus females (Figure 3F). Several windows from 1.0 – 2.0 Mb exceeded the genome-wide 95th percentile of dwarf male vs female F_{ST} with F_{ST} values between 0.21 - 0.32. F_{ST} values of 0.3 are expected for fully sex-linked regions (i.e. male XY and female XX). No such distinct pattern was observed for bourgeois males versus females (Wilcoxon rank sum test $p = 0.83$; Figure 3E) but one window with F_{ST} of 0.49 was found around 2.3 Mb that was higher between bourgeois males and females and exceeded the genome-wide 95th percentile. We also compared F_{ST} between bourgeois males and dwarf males on scaffold 23 to identify intrasexual differentiation in the sex-determining region (Figure S8). The most significant F_{ST} between the two male-types was in windows spanning 1.08 – 1.11 Mb with $F_{ST} = 0.49$ (Grubbs's outlier test $p < 6.3e\text{-}^{11}$), which also exceeded the 95th percentile of genome-wide F_{ST}. There were also 20 other F_{ST} outliers (> genome-wide 95th percentile) spread across scaffold_23.

Recombination suppression on scaffold_23

The sexual antagonism model of sex chromosome evolution posits that recombination suppression between the sex-determining loci and sexually antagonistic loci ensures that they co-segregate (D. Charlesworth & Charlesworth, 1980; Rice, 1987). To determine whether there is recombination suppression on scaffold_23, we calculated r^2 in order to quantify linkage disequilibrium (LD) using all the SNPs from all *L. callipterus* samples across scaffold_23. It is important to note that high LD can result from either recombination suppression or strong selection. We identified eight LD blocks on scaffold_23, of which

1365294x, ja, Downloaded from https://onlinelibrary.wiley.com/doi/10.1111/mec.16839 by Universität Bern, Wiley Online Library on [10/01/2023]. See the Terms and Conditions (https://onlinelibrary.wiley.com/terms-and-conditions) on Wiley Online Library for rules of use; OA articles are governed by the applicable Creative Commons License

seven blocks were < 0.03 Mb in size (Figure S9). The largest LD block, denoted LD-Block 5, was found between 1.0 – 1.4 Mb (Figure 4A). Thus, LD-Block-5 was perfectly centred around the above-mentioned regions of reduced M:F coverage and elevated F_{ST}. The pattern of LD was a V-shaped, with the centre point of the 'V' in high LD with upstream and downstream SNPs, extending from 1bp – 1.4 Mb. But the upstream and downstream SNPs were not in LD with each other. Inversions can produce high LD by restricting recombination during sex chromosomes evolution. However, we did not find evidence of inversions on scaffold_23 using two different bioinformatics approaches (see Methods). Our negative results could just reflect the limitation of the short-read data for identifying inversions. However, the LD pattern of inversions is expected to be more block-like and not 'V' shaped as we observe in our data.

Identification of candidate sex determination and body size genes on scaffold_23

By investigating the function of genes in the sex-linked regions of scaffold_23 using www.genecards.org and a thorough literature review, we identified several genes that have known functions associated with sexual development, growth, and alternative reproductive behaviours (Table 2, File S2). The 1.18 – 1.28 Mb region with the lowest M:F coverage in *L. callipterus* had two annotated genes (Table 2, File S2). One was *pituitary adenylate cyclase-activating polypeptide type I receptor* (ADCYAP1R1), a receptor of the well characterised adenylate cyclase-activating polypeptide gene (ADCYAP, alias PACAP). ADCYAP1 was located just downstream at 1.8 Mb, within the LD-Block 5 (File S2). Both this gene and its receptors are expressed in a wide variety of tissues, including the testes and ovaries (Vaudry et al., 2009) and are involved in oogenesis (Apa et al., 1997) and spermatogenesis in rats (Romanelli, Fillo, Isidori, & Conte, 1997).

Accepted Article

1365294x, ja, Downloaded from https://onlinelibrary.wiley.com/doi/10.1111/mec.16839 by Universität Bern, Wiley Online Library on [10/01/2023]. See the Terms and Conditions (https://onlinelibrary.wiley.com/terms-and-conditions) on Wiley Online Library for rules of use; OA articles are governed by the applicable Creative Commons License

Accepted Article

Located 9.9 kb upstream of ADCYAP1R1 between 1.14 – 1.18 Mb was the *growth hormone releasing hormone receptor* (GHRHR), which is a G-protein coupled receptor (GPCR) and an important player in stimulating growth hormone synthesis and secretion from the pituitary gland (Lee et al., 2007) (Figure 4, Table 2, File S2). GHRHR was found in the elevated F_{ST} region of > 0.2 between dwarf males and females (Figure 3F), and it had an F_{ST} of 0.31 between dwarf and bourgeois males (Figure S8). Mutations of GHRHR cause pituitary Dwarfism of Sindh people in a remote population of Pakistanis belonging to the Sindhi ethnic group and the *little* phenotype in laboratory mice (Baumann & Maheshwari, 1997; Godfrey et al., 1993). Thus, GHRHR is a strong candidate for body-size determination in *L. callipterus*. Both ADCYAP1R1 and GHRHR are in high LD with the genes at the centre of LD-Block 5 (Figure 4), and they also known to interact directly in protein-protein interaction networks in humans (Figure S10).

There were 15 genes in LD-Block 5, with two genes (THEM6 precursor and THEM6 (2 of 2)) at the centre of perfect LD at ~1.1 Mb (Table 2, File S2). Just upstream of THEM6 (2 of 2) lies THEM6 (1 of 2). All three of these genes are members of the thioesterase superfamily, which has been associated with regulating energy expenditure in animals (Zhang et al., 2012). A detailed discussion of other interesting genes in the LD-block can be found in the Supplementary Results and Discussion.

Turnover of sex chromosomes in the Lamprologini

L. callipterus belongs to a large, substrate-breeding clade of cichlids in Lake Tanganyika constituting the tribe Lamprologini, where shell-brooding and small body-size, particularly in females, have co-evolved multiple, independent times (Sato & Gashagaza 1997; Schütz et al. 2006; Koblmüller et al. 2007). To resolve the evolutionary history of the sex-linked region, we compared the phylogeny of the scaffold_23 sex-linked region to the whole-genome phylogeny for *L. callipterus* and six other Lamprologini species sequenced in this study

1365294x, ja, Downloaded from https://onlinelibrary.wiley.com/doi/10.1111/mec.16839 by Universität Bern, Wiley Online Library on [10/01/2023]. See the Terms and Conditions (https://onlinelibrary.wiley.com/terms-and-conditions) on Wiley Online Library for rules of use; OA articles are governed by the applicable Creative Commons License

(Table 1). The whole-genome phylogeny was constructed using 11,855 genes across the genome, and it confirmed the strongly supported (Boostrap values = 100) monophyly of all included species (Figure 5). The tree suggests that obligate shell-brooding evolved three times in these species, or that it evolved in the common ancestor of these species after it split from *N. brichardi* and was subsequently lost three times.

In the phylogeny of the candidate body-size gene, GHRHR (Figure 5 inset), the species monophyly is maintained but the position of *L. lemairii* (facultative shell-brooder) and *L. callipterus* is switched compared to the whole-genome phylogeny. This results in a cluster of all obligate-shell brooders, except for *N. brevis*. The *A. calvus* 'Congo', which is not a shell-brooder is also in this cluster. The switch in topology between the whole-genome phylogeny and the sex-region phylogeny could reflect either the coalescent history of this region or introgression. In fact, F1 hybrids between *L. callipterus* and other snail shell dwellers have been observed in nature (Koblmüller et al., 2007).

To determine whether the sex determination system in *L. callipterus* is shared with other Lamprologini, we placed the *L. callipterus* sex-linked region in a phylogenomic context by analysing the coverage of scaffold_23 in males and females of four related species (Figure S11). The facultative shell brooders *N. multifasciatus* and *L. lemarii* did not have outlier coverage windows (below the genome-wide 5th percentile) on scaffold_23. The obligate shell-brooders *L. ocellatus* had reduced coverage (below the genome-wide 5th percentile) on scaffold_23 from 1.29 to 1.34 Mb (Figure S11), but this does not overlap with the region of reduced coverage in *L. callipterus* at 1.18 – 1.28 Mb. However, it may belong to the putatively larger sex region of *L. callipterus* that was identified by re-mapping the data to the *O. niloticus* reference genome (Figure S2, S3). Two copies of the chemokine receptors XCR1B.3 are found on scaffold_23: 1.29 to 1.34 Mb. XCR1B.3 is a member of the GPCR signaling pathway that also includes ADCYAP1R1 and GHRHR. *N. brevis*, an ancestral obligate shell-brooder, had outlier windows of coverage at scaffold_23: 2.14 – 2.16 Mb, a

Accepted Article

1365294x, ja, Downloaded from https://onlinelibrary.wiley.com/doi/10.1111/mec.16839 by Universität Bern, Wiley Online Library on [10/01/2023]. See the Terms and Conditions (https://onlinelibrary.wiley.com/terms-and-conditions) on Wiley Online Library for rules of use; OA articles are governed by the applicable Creative Commons License

region devoid of genes. Overall, these observations point towards a possible shared sex-determining region on scaffold_23 in the shell-brooding Lamprologini tribe, which needs to be further investigated in a follow-up study.

No evidence for rapid evolution of the *GHRHR* gene across the lamprologini

We screened the *GHRHR* gene for signatures of selection and found evidence for purifying selection (dN/dS < 1) in all the ingroup species (*L. callipterus*, *A. calvus* 'Congo', *A.* sp. 'Sumbu shell', *L. ocellatus*) compared to the *L. lemairii* outgroup (Table S2). All ingroup species were obligate shell-brooders, with the exception of *A.* sp. 'Calvus Congo', a sister species of *A.* sp. 'Sumbu shell'. The strongest purifying selection was in the *L. callipterus* lineage (dN/dS = 0.069). This was significantly lower than the other species (*p* values = 4.0e-8; 1.19e-10; 7.0e-6 Welch's t-tests; see Table S2), which had dN/dS values greater than 0.12. We found no male specific non-synonymous mutations in the GHRHR gene, but we did identify two synonymous mutations (Figure S12). It may be that gene regulation and not sequence variation in GHRHR is controlling body-size determination in *L. callipterus*. In the future it would be valuable to study the gene expression networks and alternative splicing patterns of candidate sex and body-size genes of *L. callipterus* (Singh & Ahi, 2022; Tian et al., 2019).

Discussion

The shell-brooding cichlid species, *L. callipterus*, is a unique system to test the sexual antagonism hypothesis of sex chromosome evolution. The presence of bourgeois and dwarf male morphs that are strictly paternally inherited also offers the opportunity to study origins of Y haplotype diversity. Here we present first insights into the genomic basis of sex-linked body-size determination in *L. callipterus*, which is under sexually antagonistic selection and

Accepted Article

1365294x, ja, Downloaded from https://onlinelibrary.wiley.com/doi/10.1111/mec.16839 by Universität Bern, Wiley Online Library on [10/01/2023]. See the Terms and Conditions (https://onlinelibrary.wiley.com/terms-and-conditions) on Wiley Online Library for rules of use; OA articles are governed by the applicable Creative Commons License

Accepted Article

the foundation of two very different alternative male reproductive tactics. We identify a small sex region in *L. callipterus*, with candidate genes for sex-determination and sexual antagonism (Figure 6) and report the presence of two distinct Y haplotypes. We hypothesize that the *L. callipterus* sex chromosome may have evolved to resolve sexual antagonism over body size in males and females, followed by the evolution of Y-haplotype diversity that gave rise to two male reproductive tactics.

L. callipterus has a young sex chromosome

Using multiple lines of evidence (coverage, SNP density, LD, F_{ST}) we found scaffold_23 to be the most promising sex-linked region of *L.* callipterus (Figure 6). Consistent with expectations of recombination suppression and Y differentiation, we found a decrease in M:F coverage at scaffold_23:1.18 – 1.28 Mb and elevated LD across scaffold_23:1.0 – 1.4Mb. This decrease in coverage and increase in LD was found in both bourgeois and dwarf males supporting a shared Y region in *L. callipterus* male morphs. We also observed locally restricted decreases in male-specific SNPs in dwarf and bourgeois males on scaffold_23 between 1bp to 2.4 Mb, which is consistent with deletions on the Y chromosome (Darolti et al., 2019). In addition, we found elevated F_{ST} between dwarf males and females from 1 bp – 2.4 Mb. Higher genetic differentiation is predicted around sexually antagonistic loci that are linked to sex-determining loci (Kasimatis, Nelson, & Phillips, 2017; Kirkpatrick & Guerrero, 2014), but high F_{ST} can arise as a result of several other factors (Bissegger, Laurentino, Roesti, & Berner, 2020; Rowe, Chenoweth, & Agrawal, 2018). Overall, the differentiation in the sex-linked region of *L. callipterus* was not as extreme as that found in older therian sex chromosomes (Vicoso, 2019) probably because it is a comparatively younger sex chromosome that evolved < 3MYA (Irisarri, Singh et al., 2018). In the context of East African cichlid radiation, however, the *L. callipterus* sex region would be considered old and thus shows more differentiation than that observed in other studied cichlid sex chromosomes (Gammerdinger & Kocher, 2018). Interestingly, scaffold_23 of *L. callipterus* maps to linkage group 18, which is one of the candidate sex chromosomes of the riverine

1365294x, ja, Downloaded from https://onlinelibrary.wiley.com/doi/10.1111/mec.16839 by Universität Bern, Wiley Online Library on [10/01/2023]. See the Terms and Conditions (https://onlinelibrary.wiley.com/terms-and-conditions) on Wiley Online Library for rules of use; OA articles are governed by the applicable Creative Commons License

cichlid *Astatotilapia burtoni* (Böhne, Wilson, Postlethwait, & Salzburger, 2016; N. B. Roberts et al., 2016). Since scaffold_23 is a smaller scaffold that has been anchored to a larger linkage group in the high-quality cichlid reference genome of *Oreochromis niloticus*, by re-mapping our data to *O. niloticus* we found that scaffold_23 may be a subset of a putatively larger sex region. In future studies it would be important to generate long read data for *L. callipterus* to enhance the resolution of its sex region.

As no orthologs of known sex-determining genes such as SRY or Dmrt1 (Doris Bachtrog, 2013) were found in the *L. callipterus* sex-linked region, we determined ADCYAP1R1 as the best candidate for the master sex-determining gene due to its role in gametogenesis (Apa et al., 1997; Romanelli et al., 1997; Vaudry et al., 2009). The location of ADCYAP1R1 in the most degenerated region of scaffold_23 (1.18 – 1.28 Mb) is consistent with predictions that a novel sex-determining gene can initiate sex-chromosome evolution and differentiation. This would point to a dosage dependent mechanism, whereby fish with two copies become female and fish with one copy become male (unless there are actually more copies of this gene). This is very different from most sex-determination loci identified so far in fish, which are either genes that have divergent alleles on the X and Y chromosomes or Y-specific gene duplications (Pan et al., 2021). However, Y-specific gene duplications cannot be identified by our analytic approach, which mapped reads to the reference genome. The ADCYAP1R1 gene is a receptor of the ADCYAP gene, which has sex-specific expression associated with sexual behaviour in nest-building versus non-nest building males and female oocyte maturation in gourami fish (Levy & Degani, 2012). ADCYAP1 was located just downstream at 1.8 Mb on scaffold_23 (Table 2, File S2). Given how remarkably conserved this gene family is across vertebrates (Vaudry et al., 2009), it is likely that ADCYAP1R1 and ADCYAP1 play a functionally conserved role in *L. callipterus* sexual development. However, more detailed work is needed to determine whether and how these genes contribute to sex determination in *L. callipterus*.

Accepted Article

1365294x, ja, Downloaded from https://onlinelibrary.wiley.com/doi/10.1111/mec.16839 by Universität Bern, Wiley Online Library on [10/01/2023]. See the Terms and Conditions (https://onlinelibrary.wiley.com/terms-and-conditions) on Wiley Online Library for rules of use; OA articles are governed by the applicable Creative Commons License

Accepted Article

Linkage between the sex-determining locus and a candidate sexually-antagonistic locus

The *L. callipterus* candidate sex-determining gene, ADCYAP1R1, was in linkage with the candidate gene for body-size determination, GHRHR (Figure 4, 6). The sexual antagonism model of sex chromosome evolution postulates that novel sex determination genes may arise in response to conflict between sexes over traits such as body size (van Doorn & Kirkpatrick, 2007). Since differences in body size between males and females affect reproductive fitness in the shell-brooding *L. callipterus* (Schütz & Taborsky 2000, 2005; Schütz et al. 2006) and higher dwarf male-female F_{ST} (a possible indicator of antagonism) was found in the sex-determining region with the candidate body-size gene (Figure 6), we propose that sexual antagonism over body-size may have driven the evolution of a novel sex chromosome in *L. callipterus*. It is possible that this sex chromosome on scaffold_23 is ancestral to the lamprologini cichlid tribe, but our results were unclear (Figures S7). We also cannot rule out that it may have arisen in the lamprologini ancestor and subsequently lost in some species.

Although inversions are often found on sex chromosomes and are proposed to mediate recombination suppression (Lahn & Page, 1999; Peichel et al., 2020; Ponnikas et al., 2018), we did not find evidence of an inversion. It is possible that strong selection for low recombination facilitated the establishment of sex-specific and morph-specific polymorphisms as observed with guppy alternative male morphs (Bergero, Gardner, Bader, Yong, & Charlesworth, 2019; Sandkam et al., 2021). The region of high LD on scaffold_23 in *L. callipterus* extended beyond the sex-determining gene and the sexually antagonistic body size gene to include several other candidate genes for traits, such as behaviour, physiology, and morphology, that differentiate the *L. callipterus* male morphs (see Supplementary Results and Discussion). These behavioural, physiological, and morphological loci are likely

1365294x, ja, Downloaded from https://onlinelibrary.wiley.com/doi/10.1111/mec.16839 by Universität Bern, Wiley Online Library on [10/01/2023]. See the Terms and Conditions (https://onlinelibrary.wiley.com/terms-and-conditions) on Wiley Online Library for rules of use; OA articles are governed by the applicable Creative Commons License

co-segregating with the sex-determining locus. Thus, the sex-linked region of *L. callipterus* may govern multiple sex and male morph-related phenotypes, consistent with 'supergene' architectures found in other species with alternative male reproductive tactics (Sandkam et al., 2021; Schwander, Libbrecht, & Keller, 2014; Thompson & Jiggins, 2014).

Male morphs are associated with two Y-haplotypes

While the sex region on scaffold_23 was shared by both *L. callipterus* male morphs, there were clear differences in this region between the two males, suggesting that there are two distinct Y haplotypes in *L. callipterus* (Figure 3). The bourgeois males have an additional region of low coverage on scaffold_36 that is not found in dwarf males, which further supports that there are two distinct Y haplotypes. Within the shared sex region on scaffold_23, the dwarf male Y haplotype has lower coverage and may therefore be more degenerated than the bourgeois male Y haplotype, which can have important gene dosage effects (Raznahan et al., 2018). F_{ST} patterns across the sex region also suggested that the region of recombination suppression is larger in the dwarf male Y haplotype compared to bourgeois males. This would be the case if selection for linkage was stronger between the sex determining locus and a sexually antagonistic locus in dwarf males, perhaps because the dwarf male body size was under stronger selection pressure than the bourgeois male body size. This is conceivable as the dwarf male mating tactic is strictly applicable for males small enough to enter the shell and wriggle past the female (Sato et al. 2004), whereas the bourgeois male mating tactic may be applied by males of a range of body sizes, even if passing a size threshold to carry shells greatly improves the efficiency of this mating tactic (Schütz & Taborsky 2005). It is also possible that the much smaller population size of dwarf males compared to bourgeois males (Wirtz-Ocana et al., 2014) resulted in greater Y degeneration. Indeed, differences in the rate and extent of Y degeneration has been observed in two closely related stickleback species that share the same ancestral Y

Accepted Article

1365294x, ja, Downloaded from https://onlinelibrary.wiley.com/doi/10.1111/mec.16839 by Universität Bern, Wiley Online Library on [10/01/2023]. See the Terms and Conditions (https://onlinelibrary.wiley.com/terms-and-conditions) on Wiley Online Library for rules of use; OA articles are governed by the applicable Creative Commons License

chromosome, with more rapid and extensive degeneration in the species with the smaller effective population size (Sardell, Josephson, Dalziel, Peichel, & Kirkpatrick, 2021).

But how did the second Y haplotype evolve and how is it maintained in the population? Given that the reproductive potential and evolutionary fitness of the dwarf males is critically dependent on the fitness of the bourgeois males, we hypothesise that the bourgeois male type is ancestral. It is possible that a mutation in the GHRHR candidate body size gene gave rise to dwarf males that had higher fitness due to their efficient parasitic reproductive tactic (Michael Taborsky et al., 2018; Wirtz-Ocana et al., 2014). This high fitness allowed the new dwarfism mutation to establish and be maintained by negative frequency-dependent selection in the population (Clark, 1987; Gadgil, 1972), as the fitness of each type of males is dependent on their relative frequency in the population (M Taborsky & Brockmann, 2010; Michael Taborsky, 2008; von Kuerthy, Ros, & Taborsky, 2016). Such Y haplotype diversity has also been observed in guppies (*Poecilia reticulata*) that experience negative frequency-dependent selection on Y-linked colour patterns, as well as in the closely-related species *P. parae* in which there are five behaviourally and morphologically distinct reproductive male morphs that each have a distinct Y-haplotype (Almeida et al., 2020; Sandkam et al., 2021).

Conclusion

In conclusion, our study reveals a young sex chromosome in the Lake Tanganyika cichlid adaptive radiation that supports the sexual antagonism model of sex chromosome evolution. Our results suggest that the suite of complex traits that differ between the bourgeois and dwarf male morphs in body size, growth rate, testis/sperm size, behaviour and reproductive strategy are delineated by two distinct Y haplotypes. Future functional studies of candidate genes and long-read exploration of the *L. callipterus* sex-linked region provide exciting avenues to further investigate the sexual antagonism hypothesis and the evolution of male alternative reproductive tactics.

Accepted Article

1365294x, ja, Downloaded from https://onlinelibrary.wiley.com/doi/10.1111/mec.16839 by Universität Bern, Wiley Online Library on [10/01/2023]. See the Terms and Conditions (https://onlinelibrary.wiley.com/terms-and-conditions) on Wiley Online Library for rules of use; OA articles are governed by the applicable Creative Commons License

Accepted Article

1365294x, ja, Downloaded from https://onlinelibrary.wiley.com/doi/10.1111/mec.16839 by Universität Bern, Wiley Online Library on [10/01/2023]. See the Terms and Conditions (https://onlinelibrary.wiley.com/terms-and-conditions) on Wiley Online Library for rules of use; OA articles are governed by the applicable Creative Commons License

References

Almeida, P., Sandkam, B., Morris, J., Darolti, I., Breden, F., & Mank, J. (2020). Divergence and remarkable diversity of the Y chromosome in guppies. *Molecular Biology and Evolution*, 1–38. doi: 10.1101/2020.07.13.200196

Apa, R., Lanzone, A., Mastrandrea, M., Miceli, F., Macchione, E., Fulghesu, A., … Canipari, R. (1997). Effect of pituitary adenylate cyclase-activating peptide on meiotic maturation in follicle-enclosed, cumulus-enclosed, and denuded rat oocytes. *Biology of Reproduction*, *57*, 1074–1079.

Bachtrog, D., Mank, J. E., Peichel, C. L., M., K., Otto, S. P., Ashman, T. L., … Vamosi, J. C. (2014). Sex determination: why so many ways of doing it? *PLoS Biology*, *12*(7), e1001899. doi: 10.1371/journal.pbio.1001899

Bachtrog, Doris. (2013). Y-chromosome evolution: emerging insights into processes of Y-chromosome degeneration. *Nature Reviews Genetics*, *14*(2), 113–124. doi: 10.1038/nrg3366

Baumann, G., & Maheshwari, H. (1997). The Dwarfs of Sindh: severe growth hormone (GH) deficiency caused by a mutation in the GH-releasing hormone receptor gene. *Acta Paediatrica*, *423*, 33–38.

Bergero, R., Gardner, J., Bader, B., Yong, L., & Charlesworth, D. (2019). Exaggerated heterochiasmy in a fish with sex-linked male coloration polymorphisms. *PNAS*, *116*(14), 6924–6931. doi: 10.1073/pnas.1818486116

Bissegger, M., Laurentino, T. G., Roesti, M., & Berner, D. (2020). Widespread intersex differentiation across the stickleback genome – The signature of sexually antagonistic selection? *Molecular Ecology*, *29*(2), 262–271. doi: 10.1111/mec.15255

Böhne, A., Wilson, C. A., Postlethwait, J. H., & Salzburger, W. (2016). Variations on a theme: genomics of sex determination in the cichlid fish Astatotilapia burtoni. *BMC Genomics*, *17*(883), 1–12. doi: 10.1186/s12864-016-3178-0

Brawand, D., Wagner, C. E., Li, Y. I., Malinsky, M., Keller, I., Fan, S., … Di Palma, F. (2014). The genomic substrate for adaptive radiation in African cichlid fish. *Nature*, *513*, 375–381. doi: 10.1038/nature13726

Brockmann, H.J. & Taborsky, M. (2008). Alternative reproductive tactics and the evolution of alternative allocation phenotypes. In *Alternative Reproductive Tactics: An integrative approach* (pp. 25–51). Cambridge: Cambridge University Press.

Charlesworth, B., & Charlesworth, D. (2000). The degeneration of Y chromosomes. *Philosophical Transactions of the Royal Society B: Biological Sciences*, *355*(1403), 1563–1572. doi: 10.1098/RSTB.2000.0717

Charlesworth, Brian. (1996). The evolution of chromosomal sex determination and dosage compensation. *Current Biology*, *6*, 149–162.

Charlesworth, D., & Charlesworth, B. (1980). Sex differences in fitness and selection for centric fusions between sex-chromosomes and autosomes. *Genet. Res., Camb*, *35*, 205–214. doi: 10.1017/S0016672300014051

Charlesworth, D., Charlesworth, B., & Marais, G. (2005). Steps in the evolution of heteromorphic sex chromosomes. *Heredity*, *95*(2), 118–128. doi: 10.1038/sj.hdy.6800697

Clark, A. G. (1987). Natural selection and Y-linked polymorphism. *Genetics*, *115*(3), 569–577. Retrieved from https://pubmed.ncbi.nlm.nih.gov/3569883

Conte, M. A., Gammerdinger, W. J., Bartie, K. L., Penman, D. J., & Kocher, T. D. (2017). A high quality assembly of the Nile Tilapia (Oreochromis niloticus) genome reveals the structure of two sex determination regions. *BMC Genomics*, *18*(1), 1–19. doi: 10.1186/S12864-017-3723-5/TABLES/9

Darolti, I., & Mank, J. E. (2022). A bioinformatic toolkit to simultaneously identify sex and sex-linked regions. *Molecular Ecology Resources*, *22*(2), 455–457. doi: 10.1111/1755-0998.13530

Darolti, I., Wright, A. E., Sandkam, B. A., Morris, J., Bloch, N. I., Farré, M., … Mank, J. E. (2019). Extreme heterogeneity in sex chromosome differentiation and dosage

Accepted Article

1365294x, ja, Downloaded from https://onlinelibrary.wiley.com/doi/10.1111/mec.16839 by Universität Bern, Wiley Online Library on [10/01/2023]. See the Terms and Conditions (https://onlinelibrary.wiley.com/terms-and-conditions) on Wiley Online Library for rules of use; OA articles are governed by the applicable Creative Commons License

compensation in livebearers. *PNAS*, *116*(38), 19031–19036. doi: 10.1073/pnas.1905298116

El Taher, A., Böhne, A., Boileau, N., Ronco, F., Indermaur, A., Widmer, L., & Salzburger, W. (2021). Gene expression dynamics during rapid organismal diversification in African cichlid fishes. *Nature Ecology & Evolution*, *5*(2), 243–250. doi: 10.1038/s41559-020-01354-3

Fontaine, A., Filipović, I., Fansiri, T., Hoffmann, A. A., Cheng, C., Kirkpatrick, M., … Lambrechts, L. (2017). Extensive genetic differentiation between homomorphic sex chromosomes in the mosquito vector, Aedes aegypti. *Genome Biology and Evolution*, *9*(9), 2322–2335. doi: 10.1093/gbe/evx171

Gadgil, M. (1972). Male dimorphism as a consequence of sexual selection. *The American Naturalist*, *106*(951), 574–580. Retrieved from http://www.jstor.org/stable/2459720

Gammerdinger, W. J., Conte, M. A., Acquah, E. A., Roberts, R. B., & Kocher, T. D. (2014). Structure and decay of a proto-Y region in Tilapia, Oreochromis niloticus. *BMC Genomics*, *15*(1–9). doi: 10.1186/1471-2164-15-975

Gammerdinger, W. J., & Kocher, T. D. (2018). Unusual diversity of sex chromosomes in African cichlid fishes. *Genes*, *9*(480), 1–20. doi: 10.3390/genes9100480

Godfrey, P., Rahal, J. O., Beamer, W. G., Copeland, N. G., Jenkins, N. A., & Mayo, K. E. (1993). GHRH receptor of little mice contains a missense mutation in the extracellular domain that disrupts receptor function. *Nature Genetics*, *4*(3), 227–232. doi: 10.1038/ng0793-227

Irisarri, I., Singh, P., Koblmüller, S., Torres-Dowdall, J., Henning, F., Franchini, P., … Meyer, A. (2018). Phylogenomics uncovers early hybridization and adaptive loci shaping the radiation of Lake Tanganyika cichlid fishes. *Nature Communications*, *9*(3159), 1–12. doi: 10.1038/s41467-018-05479-9

Ironside, J. E. (2010). No amicable divorce? Challenging the notion that sexual antagonism drives sex chromosome evolution. *BioEssays*, *32*(8), 718–726. doi: 10.1002/bies.200900124

Accepted Article

1365294x, ja, Downloaded from https://onlinelibrary.wiley.com/doi/10.1111/mec.16839 by Universität Bern, Wiley Online Library on [10/01/2023]. See the Terms and Conditions (https://onlinelibrary.wiley.com/terms-and-conditions) on Wiley Online Library for rules of use; OA articles are governed by the applicable Creative Commons License

Kasimatis, K. R., Nelson, T. C., & Phillips, P. C. (2017). Genomic Signatures of Sexual Conflict. *Journal of Heredity*, *108*(7), 780–790. doi: 10.1093/jhered/esx080

Kim, S. A., Brossard, M., Roshandel, D., Paterson, A. D., Bull, S. B., & Yoo, Y. J. (2019). gpart: human genome partitioning and visualization of high-density SNP data by identifying haplotype blocks. *Bioinformatics*, *35*(21), 4419–4421. doi: 10.1093/bioinformatics/btz308

Kirkpatrick, M., & Guerrero, R. F. (2014). Signatures of sex-antagonistic selection on recombining sex chromosomes. *Genetics*, *197*(2), 531–541. doi: 10.1534/genetics.113.156026

Kitano, J., Ross, J. A., Mori, S., Kume, M., Jones, F. C., Chan, Y. F., … Peichel, C. L. (2009). A role for a neo-sex chromosome in stickleback speciation. *Nature*, *461*(7267), 1079–1083. doi: 10.1038/nature08441

Ko, C., Gieske, M. C., Al-Alem, L., Hahn, Y., Su, W., Gong, M. C., … Koo, Y. (2006). Endothelin-2 in ovarian follicle rupture. *Endocrinology*, *147*(4), 1770–1779. doi: 10.1210/en.2005-1228

Koblmüller, S., Duftner, N., Sefc, K. M., Aibara, M., Stipacek, M., Blanc, M., … Sturmbauer, C. (2007). Reticulate phylogeny of gastropod-shell-breeding cichlids from Lake Tanganyika-the result of repeated introgressive hybridization. *BMC Evolutionary Biology*, *7*(7), 1–13. doi: 10.1186/1471-2148-7-7

Korneliussen, T. S., Albrechtsen, A., & Nielsen, R. (2014). ANGSD: analysis of next generation sequencing data. *BMC Bioinformatics*, *15*(356).

Lahn, B. T., & Page, D. C. (1999). Four Evolutionary Strata on the Human X Chromosome. *Science*, *286*(5441), 964–967. doi: 10.1126/science.286.5441.964

Lande, R., Seehausen, O., & Van Alphen, J. J. M. (2001). Mechanisms of rapid sympatric speciation by sex reversal and sexual selection in cichlid fish. *Genetica*, *112*, 435–443.

Langmead, B., Trapnell, C., Pop, M., & Salzberg, S. L. (2009). Ultrafast and memory-efficient alignment of short DNA sequences to the human genome. *Genome Biology*, *10*(3), R25. doi: 10.1186/gb-2009-10-3-r25

Accepted Article

1365294x, ja, Downloaded from https://onlinelibrary.wiley.com/doi/10.1111/mec.16839 by Universität Bern, Wiley Online Library on [10/01/2023]. See the Terms and Conditions (https://onlinelibrary.wiley.com/terms-and-conditions) on Wiley Online Library for rules of use; OA articles are governed by the applicable Creative Commons License

Layer, R. M., Chiang, C., Quinlan, A. R., & Hall, I. M. (2014). LUMPY: a probabilistic framework for structural variant discovery. *Genome Biology*, *15*(6), 1–19. doi: 10.1186/gb-2014-15-6-r84

Lee, L. T. O., Siu, F. K. Y., Tam, J. K. V., Lau, I. T. Y., Wong, A. O. L., Lin, M. C. M., … Chow, B. K. C. (2007). Discovery of growth hormone-releasing hormones and receptors in nonmammalian vertebrates. *PNAS*, *104*(7), 2133–2138. doi: 10.1073/pnas.0611008104

Levy, G., & Degani, G. (2012). Involvement of GnRH, PACAP and PRP in the reproduction of blue gourami females (Trichogaster trichopterus). *Journal of Molecular Neuroscience*, *48*(3), 603–616. doi: 10.1007/s12031-012-9730-8

Li, H., Handsaker, B., Wysoker, A., Fennell, T., Ruan, J., Homer, N., … Durbin, R. (2009). The Sequence Alignment/Map format and SAMtools. *Bioinformatics*, *25*(16), 2078–2079. doi: 10.1093/bioinformatics/btp352

Mirarab, S., & Warnow, T. (2015). ASTRAL-II: coalescent-based species tree estimation with many hundreds of taxa and thousands of genes. *Bioinformatics*, *31*(12), i44–i52.

Ozouf-Costaz, C., Coutanceau, J.-P., Bonillo, C., Mercot, H., Fermon, Y., & Guidi-Rontani, C. (2017). New insights into the chromosomal differentiation patterns among cichlids from Africa and Madagascar. *Cybium*, *41*(1), 35–43.

Palmer, D. H., Rogers, T. F., Dean, R., & Wright, A. E. (2019). How to identify sex chromosomes and their turnover. *Molecular Ecology*, *28*(21), 4709–4724. doi: 10.1111/mec.15245

Pan, Q., Kay, T., Depincé, A., Adolfi, M., Schartl, M., Guiguen, Y., & Herpin, A. (2021). Evolution of master sex determiners: TGF-β signalling pathways at regulatory crossroads. *Proc. R. Soc. B*. doi: 10.1098/rstb.2020.0091

Parker, G. A. (1984). *Evolutionarily stable strategies. In Behavioural ecology: an evolutionary approach* (2nd ed.; J. R. Krebs & N. B. Davies, eds.). Sinauer Associates, Sunderland, MA.

Peichel, C. L., McCann, S. R., Ross, J. A., Naftaly, A. F. S., Urton, J. R., Cech, J. N., …

Accepted Article

1365294x, ja, Downloaded from https://onlinelibrary.wiley.com/doi/10.1111/mec.16839 by Universität Bern, Wiley Online Library on [10/01/2023]. See the Terms and Conditions (https://onlinelibrary.wiley.com/terms-and-conditions) on Wiley Online Library for rules of use; OA articles are governed by the applicable Creative Commons License

White, M. A. (2020). Assembly of the threespine stickleback Y chromosome reveals convergent signatures of sex chromosome evolution. *Genome Biology*, *21*(1), 177. doi: 10.1186/s13059-020-02097-x

Pfeifer, B., Wittelsbürger, U., Ramos-Onsins, S. E., & Lercher, M. J. (2014). PopGenome: an efficient Swiss army knife for population genomic analyses in R. *Molecular Biology and Evolution*, *31*(7), 1929–1936. doi: 10.1093/molbev/msu136

Poletto, A. B., Ferreira, I. A., Cabral-de-Mello, D. C., Nakajima, R. T., Mazzuchelli, J., Ribeiro, H. B., … Martins, C. (2010). Chromosome differentiation patterns during cichlid fish evolution. *BMC Genetics*, *11*(1), 50. doi: 10.1186/1471-2156-11-50

Ponnikas, S., Sigeman, H., Abbott, J. K., & Hansson, B. (2018). Why do sex chromosomes stop recombining? *Trends in Genetics*, *34*(7), 492–503. doi: 10.1016/J.TIG.2018.04.001

Quinlan, A. R., & Hall, I. M. (2010). BEDTools: a flexible suite of utilities for comparing genomic features. *Bioinformatics*, *26*(6), 841–842. doi: 10.1093/bioinformatics/btq033

Rausch, T., Zichner, T., Schlattl, A., Stütz, A. M., Benes, V., & Korbel, J. O. (2012). DELLY: structural variant discovery by integrated paired-end and split-read analysis. *Bioinformatics*, *28*(18), 333–339. doi: 10.1093/bioinformatics/bts378

Raznahan, A., Parikshak, N. N., Chandran, V., Blumenthal, J. D., Clasen, L. S., Alexander-Bloch, A. F., … Geschwind, D. H. (2018). Sex-chromosome dosage effects on gene expression in humans. *PNAS*, *115*(28), 7398 LP – 7403. doi: 10.1073/pnas.1802889115

Rice, W. R. (1987). The accumulation of sexually antagonistic genes as a selective agent promoting the evolution of reduced recombination primitive sex chromosomes. *Evolution*, *41*(4), 911–914. doi: 10.1111/j.1558-5646.1987.tb05864.x

Roberts, N. B., Juntti, S. A., Coyle, K. P., Dumont, B. L., Stanley, M. K., Ryan, A. Q., … Roberts, R. B. (2016). Polygenic sex determination in the cichlid fish Astatotilapia burtoni. *BMC Genomics*, 1–13. doi: 10.1186/s12864-016-3177-1

Roberts, R. B., Ser, J. R., & Kocher, T. D. (2009). Sexual conflict resolved by invasion of a novel sex determiner in Lake Malawi cichlid fishes. *Science*, *326*(5955), 998–1001. doi:

Accepted Article

1365294x, ja, Downloaded from https://onlinelibrary.wiley.com/doi/10.1111/mec.16839 by Universität Bern, Wiley Online Library on [10/01/2023]. See the Terms and Conditions (https://onlinelibrary.wiley.com/terms-and-conditions) on Wiley Online Library for rules of use; OA articles are governed by the applicable Creative Commons License

10.1126/science.1174705

Romanelli, F., Fillo, S., Isidori, A., & Conte, D. (1997). Pituitary adenylate cyclase-activating polypeptide regulates rat Leydig cell function in vitro. *Neuropeptides*, *31*(4), 311–317. doi: 10.1016/S0143-4179(97)90064-0

Rowe, L., Chenoweth, S. F., & Agrawal, A. F. (2018). The genomics of sexual conflict. *American Naturalist*, *192*(2), 274–286. doi: 10.1086/698198

Sandkam, B. A., Almeida, P., Darolti, I., Furman, B. L. S., van der Bijl, W., Morris, J., … Mank, J. E. (2021). Extreme Y chromosome polymorphism corresponds to five male reproductive morphs of a freshwater fish. *Nature Ecology & Evolution*, *5*(7), 939–948. doi: 10.1038/s41559-021-01452-w

Sardell, J. M., Josephson, M. P., Dalziel, A. C., Peichel, C. L., & Kirkpatrick, M. (2021). Heterogeneous Histories of Recombination Suppression on Stickleback Sex Chromosomes. *Molecular Biology and Evolution*, *38*(10), 4403–4418. doi: 10.1093/MOLBEV/MSAB179

Sato, T., & Gashagaza, M. M. (1997). Shell-brooding cichlid fishes of Lake Tanganyika: Their habitats and mating systems. In M. Kawanabe, M. Hori, & M. Nagoshi (Eds.), *Fish Communities in Lake Tanganyika* (pp. 219–240). Kyoto: Kyoto University Press.

Sato, Tetsu, Hirose, M., Taborsky, M., & Kimura, S. (2004). Size-dependent male alternative reproductive tactics in the shell-brooding cichlid fish Lamprologus callipterus in Lake Tanganyika. *Ethology*, *110*, 49–62.

Schütz, D., Parker, G. A., Taborsky, M., & Sato, T. (2006). An optimality approach to male and female body sizes in an extremely size-dimorphic cichlid fish. *Evolutionary Ecology Research*, *8*, 1-1393–1408.

Schütz, D., & Taborsky, M. (2005). The influence of sexual selection and ecological constraints on an extreme sexual size dimorphism in a cichlid. *Animal Behaviour*, *70*, 539–549. doi: 10.1016/j.anbehav.2004.11.010

Schütz, D, & Taborsky, M. (2000). Giant males or dwarf females: what determines the extreme sexual size dimorphism in Lamprologus callipterus? *Journal of Fish Biology*,

Accepted Article

1365294x, ja, Downloaded from https://onlinelibrary.wiley.com/doi/10.1111/mec.16839 by Universität Bern, Wiley Online Library on [10/01/2023]. See the Terms and Conditions (https://onlinelibrary.wiley.com/terms-and-conditions) on Wiley Online Library for rules of use; OA articles are governed by the applicable Creative Commons License

57(5), 1254–1265. doi: 10.1006/jfbi.2000.1388

Schütz, Dolores, Pachler, G., Ripmeester, E., Goffinet, O., & Taborsky, M. (2010). Reproductive investment of giants and dwarfs: specialized tactics in a cichlid fish with alternative male morphs. *Functional Ecology*, *24*, 131–140. doi: 10.1111/j.1365-2435.2009.01605.x

Schwander, T., Libbrecht, R., & Keller, L. (2014). Supergenes and complex phenotypes. *Current Biology*, *24*(7), R288–R294. doi: https://doi.org/10.1016/j.cub.2014.01.056

Singh, P., & Ahi, E. P. (2022). The importance of alternative splicing in adaptive evolution. *Molecular Ecology*, *31*(7), 1928–1938. doi: 10.1111/MEC.16377

Stamatakis, A. (2014). RAxML version 8: a tool for phylogenetic analysis and post-analysis of large phylogenies. *Bioinformatics*, *30*, 1312–1313.

Taborsky, M. (2001). The evolution of bourgeois, parasitic, and cooperative reproductive behaviors in fishes. *Journal of Heredity*, *92*(2), 100–110. doi: 10.1093/jhered/92.2.100

Taborsky, M, & Brockmann, H. (2010). Alternative tactics and life history phenotypes. In *Animal behaviour: Evolution and Mechanisms* (P. M. Kapp, pp. 537–586). Berlin, Germany: Springer Verlag.

Taborsky, Michael. (1997). Bourgeois and parasitic tactics: do we need collective, functional terms for alternative reproductive behaviours? *Behavioral Ecology and Sociobiology 1997 41:5*, *41*(5), 361–362. doi: 10.1007/S002650050396

Taborsky, Michael. (2008). Alternative reproductive tactics in fish. In *Alternative reproductive tactics: an integrative approach* (pp. 251–299). Cambridge University Press.

Taborsky, Michael, Schütz, D., Goffinet, O., & Doorn, G. S. Van. (2018). Alternative male morphs solve sperm performance/longevity trade-off in opposite directions. *Science Advances*, *4*(eaap8563), 1–9.

Thompson, M. J., & Jiggins, C. D. (2014). Supergenes and their role in evolution. *Heredity*, *113*, 1–8. doi: 10.1038/hdy.2014.20

Tian, F., Liu, S., Shi, J., Qi, H., Zhao, K., & Xie, B. (2019). Transcriptomic profiling reveals molecular regulation of seasonal reproduction in Tibetan highland fish, Gymnocypris

Accepted Article

1365294x, ja, Downloaded from https://onlinelibrary.wiley.com/doi/10.1111/mec.16839 by Universität Bern, Wiley Online Library on [10/01/2023]. See the Terms and Conditions (https://onlinelibrary.wiley.com/terms-and-conditions) on Wiley Online Library for rules of use; OA articles are governed by the applicable Creative Commons License

przewalskii. *BMC Genomics*, *20*(1), 1–13. doi: 10.1186/s12864-018-5358-6

van Doorn, G. S., & Kirkpatrick, M. (2007). Turnover of sex chromosomes induced by sexual conflict. *Nature*, *449*(7164), 909–912. doi: 10.1038/nature06178

Vaudry, D., Falluel-Morel, A., Bourgault, S., Basille, M., Burel, D., Wurtz, O., … Vaudry, H. (2009). Pituitary adenylate cyclase-activating polypeptide and its receptors: 20 years after the discovery. *Pharmacological Reviews*, *61*(3), 283–357. doi: 10.1124/pr.109.001370.283

Vicoso, B. (2019). Molecular and evolutionary dynamics of animal sex-chromosome turnover. *Nature Ecology & Evolution*. doi: 10.1038/s41559-019-1050-8

von Kuerthy, C., Ros, A. F. H., & Taborsky, M. (2016). Androgen responses to reproductive competition of males pursuing either fixed or plastic alternative reproductive tactics. *Journal of Experimental Biology*, *219*(22), 3544–3553. doi: 10.1242/jeb.143974

von Kuerthy, C., & Taborsky, M. (2016). Contest versus scramble competition among males pursuing fixed or plastic alternative reproductive tactics. *Animal Behaviour*, *113*, 203–212. doi: 10.1016/J.ANBEHAV.2016.01.006

Wirtz-Ocana, S., Meidl, P., Bonfils, D., & Taborsky, M. (2014). Y-linked Mendelian inheritance of giant and dwarf male morphs in shell-brooding cichlids. *Proc. R. Soc. B*, *281*(20140253).

Wirtz-Ocana, S., Schütz, D., Pachler, G., & Taborsky, M. (2013). Paternal inheritance of growth in fish pursuing alternative reproductive tactics. *Ecology and Evolution*, *3*(6), 1614–1625. doi: 10.1002/ece3.570

Wright, A. E., Darolti, I., Bloch, N. I., Oostra, V., Sandkam, B., Buechel, S. D., … Mank, J. E. (2017). Convergent recombination suppression suggests role of sexual selection in guppy sex chromosome formation. *Nature Communications*, *8*, 14251. doi: 10.1038/ncomms14251

Yamada, K. D., Tomii, K., & Katoh, K. (2016). Application of the MAFFT sequence alignment program to large data - reexamination of the usefulness of chained guide trees. *Bioinformatics*, 1–6. doi: 10.1093/bioinformatics/btw412

Accepted Article

1365294x, ja, Downloaded from https://onlinelibrary.wiley.com/doi/10.1111/mec.16839 by Universität Bern, Wiley Online Library on [10/01/2023]. See the Terms and Conditions (https://onlinelibrary.wiley.com/terms-and-conditions) on Wiley Online Library for rules of use; OA articles are governed by the applicable Creative Commons License

Yang, Z. (2007). PAML 4: Phylogenetic analysis by maximum likelihood. *Molecular Biology and Evolution*, *24*, 1586–1591.

Zhang, Y., Li, Y., Niepel, M. W., Kawano, Y., Han, S., Liu, S., … Cohen, D. E. (2012). Targeted deletion of thioesterase superfamily member 1 promotes energy expenditure and protects against obesity and insulin resistance. *PNAS*, *109*(14), 5417–5422. doi: 10.1073/pnas.1116011109

Acknowledgements

We thank the ZMF facility at Med-Uni Graz for library preparation, W. Gessl for fish photographs and M. Koller for figure editing.

Funding

This work was supported by the Swiss National Foundation grant (SNF Project 310030B-138660) to MT and the Austrian Science Fund grant (FWF P29838) to CS. PS was funded by a PhD scholarship from the Austrian Centre of Limnology, University of Graz.

Author Contributions

MT, CS conceived the study. CLP contributed to interpretation of results. PS designed and conducted all analyses, made the figures, and drafted the manuscript, which was edited by MT, CS, CLP. All authors have read and approved the final manuscript.

Declaration of Interests

The authors declare no competing interests.

Data Availability

WGS data has been deposited to NCBI SRA (https://dataview.ncbi.nlm.nih.gov/object/PRJNA593252?reviewer=gi3t337sqe3vmb1beknpd

Accepted Article

1365294x, ja, Downloaded from https://onlinelibrary.wiley.com/doi/10.1111/mec.16839 by Universität Bern, Wiley Online Library on [10/01/2023]. See the Terms and Conditions (https://onlinelibrary.wiley.com/terms-and-conditions) on Wiley Online Library for rules of use; OA articles are governed by the applicable Creative Commons License

b9a31). Analysis code is available on https://github.com/poojasingh09/sex_chromosome_cichlid.

Figure Legends

Figure 1 The *L. callipterus* cichlid system from Lake Tanganyika and genomic patterns across male and female individuals of this species.

(A) The shell-brooding cichlid species *L. callipterus* from Lake Tanganyika in East Africa has large 'bourgeois' males that collect empty snail shells and build nests, small females that enter the snail shells to lay eggs, and even smaller dwarf males that sneak past brooding females to fertilise laid eggs in close contact. Figure adapted by P. Singh from B. Taborsky's version published in Taborsky (1998) (B) Growth and size differences between bourgeois and dwarf males during development. Figure adapted from Wirtz-Ocana et al. (2013). Normalised genome-wide coverage differentiation between (C) bourgeois males (n=2) versus females (n=4) and (E) dwarf males (n=2) versus females (n=4). Genomic coverage is calculated in 1.0 Mb windows with a step-size of 0.5 Mb. Dots represent normalised $\log_2$(average male coverage/average female coverage). Solid red/blue lines represent the moving average. Grey dashed horizontal lines represent the 1st and 99th genome-wide percentiles. Black dashed horizontal lines represent the genome-wide mean. Coloured vertical shades demarcate the proposed sex-linked region of *L. callipterus* on scaffold_23. Data from (C,E) are presented as density plots in (D, F).

Figure 2 Distribution of M:F coverage and SNP density for all scaffolds in *L. callipterus.*

Comparisons between (A) bourgeois males and females and (B) dwarf males and females. Scaffold_23 and scaffold_36 are divided based on the bimodal peaks in Figure 1D,F: windows between scaffold_23: 1 bp – 2.4 Mb are pink, windows between scaffold_23 2.4 – 6.8 Mb are black, windows between scaffold_36: 2 – 3.5 Mb are green and windows

Accepted Article

1365294x, ja, Downloaded from https://onlinelibrary.wiley.com/doi/10.1111/mec.16839 by Universität Bern, Wiley Online Library on [10/01/2023]. See the Terms and Conditions (https://onlinelibrary.wiley.com/terms-and-conditions) on Wiley Online Library for rules of use; OA articles are governed by the applicable Creative Commons License

between scaffold_36: 1bp – 2 Mb and 3.5 – 4.9 Mb are blue. Windows from all other scaffolds are grey. Circles denotes the mean and vertical and horizontal lines depict the standard deviation. Dotted lines denote coverage and SNP density means across all scaffolds.

Figure 3 Differentiation in the *L. callipterus* sex-linked region on scaffold_23.

Comparisons of bourgeois males relative to females (A,C,E) and dwarf males relative to females (B,D,F) for normalised $\log_2$ M:F coverage (A,B), $\log_2$ M:F SNP density (C,D), and weighted F_{ST} (E,F). All statistics are calculated in 30 Kb windows. Solid lines denote rolling mean. Grey dashed horizontal lines represent the 5th and 95th genome-wide percentiles. Black dashed horizontal lines represent the genome-wide mean.

Figure 4 Linkage disequilibrium (LD) measured using r^2 on scaffold_23.

(A) Heatmap of LD on part of scaffold_23 (the entire scaffold is shown in Figure S8). Identified LD blocks B1 – B5 are indicated; B5 is the largest LD block, spanning 1-1.4 Mb. (B) Genes from 1.05-1.26 Mb in LD block B5 are shown. The location of SNPs used to calculate r^2 is denoted by grey lines; location of SNPs in candidate genes for sex determination and body size is denoted by lines coloured by the gene that they are found in.

Figure 5 Whole-genome phylogeny and GHRHR gene phylogeny of lamprologine species sequenced in this study.

Main: genome-wide phylogeny. Inset: phylogeny of the GHRHR gene. Node values represent bootstrap statistics. See Table 1 for details on shell-brooding status of each species. Fish photos not to scale (© W. Gessl, University of Graz).

Accepted Article

1365294x, ja, Downloaded from https://onlinelibrary.wiley.com/doi/10.1111/mec.16839 by Universität Bern, Wiley Online Library on [10/01/2023]. See the Terms and Conditions (https://onlinelibrary.wiley.com/terms-and-conditions) on Wiley Online Library for rules of use; OA articles are governed by the applicable Creative Commons License

Figure 6 Summary of major genomic patterns found in the *L. callipterus* sex-linked region on scaffold_23 from 1 bp – 2.4 Mb.

Accepted Article

1365294x, ja, Downloaded from https://onlinelibrary.wiley.com/doi/10.1111/mec.16839 by Universität Bern, Wiley Online Library on [10/01/2023]. See the Terms and Conditions (https://onlinelibrary.wiley.com/terms-and-conditions) on Wiley Online Library for rules of use; OA articles are governed by the applicable Creative Commons License

Accepted Article

Tables

Table 1. Species, sex, average body size, and brooding strategy of individuals sequenced in this study

Species (breeding mode)	No. of samples sequenced	~Body size (cm)
Lamprologous callipterus (obligate shell-brooder)	2 bourgeois males 2 dwarf males 4 females (1 daughter per male)	12.0 3.0 6.0
Lamprologous lemairii (facultative shell-brooder)	1 male 1 female	22.0 Not known
Lamprologous ocellatus 'gold' (obligate shell-brooder)	1 male 1 female	5.0 3.5
Neolamprologous brevis (obligate shell-brooder)	1 male 1 female	6.0 4.0
Neolamprologous multifasciatus (facultative shell-brooder)	1 male 1 female	4.0 2.5
Altolamprologus sp. 'Sumbu Shell' (obligate shell-brooder)	1 male	5.5
Altolamprologus calvus 'Congo' (not a shell-brooder)	1 male	10

1365294x, ja, Downloaded from https://onlinelibrary.wiley.com/doi/10.1111/mec.16839 by Universität Bern, Wiley Online Library on [10/01/2023]. See the Terms and Conditions (https://onlinelibrary.wiley.com/terms-and-conditions) on Wiley Online Library for rules of use; OA articles are governed by the applicable Creative Commons License

Accepted Article

Table 2. List of sex and body-size relevant genes on the *L. callipterus* sex-linked region LD Block 5. For a full list of genes in the sex-linked region see File S2.

Gene position on scaffold_23	Gene name	Function or phenotype	Reference
993878 - 1034646	B4GALT1	Ehlers-Danlos progeroid syndrome (premature ageing), homologue B4GALT7 causes dwarfism in horses	Leegwater et al. 2016
1085286 - 1094884	THEM6 precursor	Regulates THEM6	
1099381-1100314	THEM6 (2 of 2)	Metabolic regulation of brown fat and energy expenditure	Zhang et al. (2012)
1107073 - 1107814	THEM6 (1 of 2)	Metabolic regulation of brown fat and energy expenditure	Zhang et al. (2012)
1125564 - 1132363	EEF1D (1 of 2)	Intellectual and adaptive functioning	Iseri et al. 2019
1137957 - 1178397	GHRHR	Growth/Dwarfism of Sindh, little mice	Godfrey et al. 1993; Baumann & Maheshwari 1997; Perry et al. 2014
1188396 - 1210632	ADCYAP1R1	Gametogenesis	Romanelli et al. 1997; Daniel & Habener 2000
1290830 - 1352831	*XCR1b.3* (2 tandem duplicates)	GPCR signalling pathway member that includes ghrhra and adcyap1r1	Fox et al. 2019
1395330 - 1484131	PDE1C	Infertility, male mating-behaviour in Drosophila	Morton et al. 2010
1842461 - 1845858	ADCYAP1	Sexual behaviour in nest-building vs non-nest building males and female oocyte maturation in gourami fish	Levy & Degani 2012

Supplementary Files

File S1 Sample relatedness calculated using SNPs.

1365294x, ja, Downloaded from https://onlinelibrary.wiley.com/doi/10.1111/mec.16839 by Universität Bern, Wiley Online Library on [10/01/2023]. See the Terms and Conditions (https://onlinelibrary.wiley.com/terms-and-conditions) on Wiley Online Library for rules of use; OA articles are governed by the applicable Creative Commons License

File S2 Detailed annotation of genes in the *L. callipterus* sex-linked region on scaffold_23: 1 bp – 2.4 Mb and scaffold_36: 2-3.5 Mb.

Supplementary Results and Discussion

Accepted Article

1365294x, ja, Downloaded from https://onlinelibrary.wiley.com/doi/10.1111/mec.16839 by Universität Bern, Wiley Online Library on [10/01/2023]. See the Terms and Conditions (https://onlinelibrary.wiley.com/terms-and-conditions) on Wiley Online Library for rules of use; OA articles are governed by the applicable Creative Commons License

Figure 1

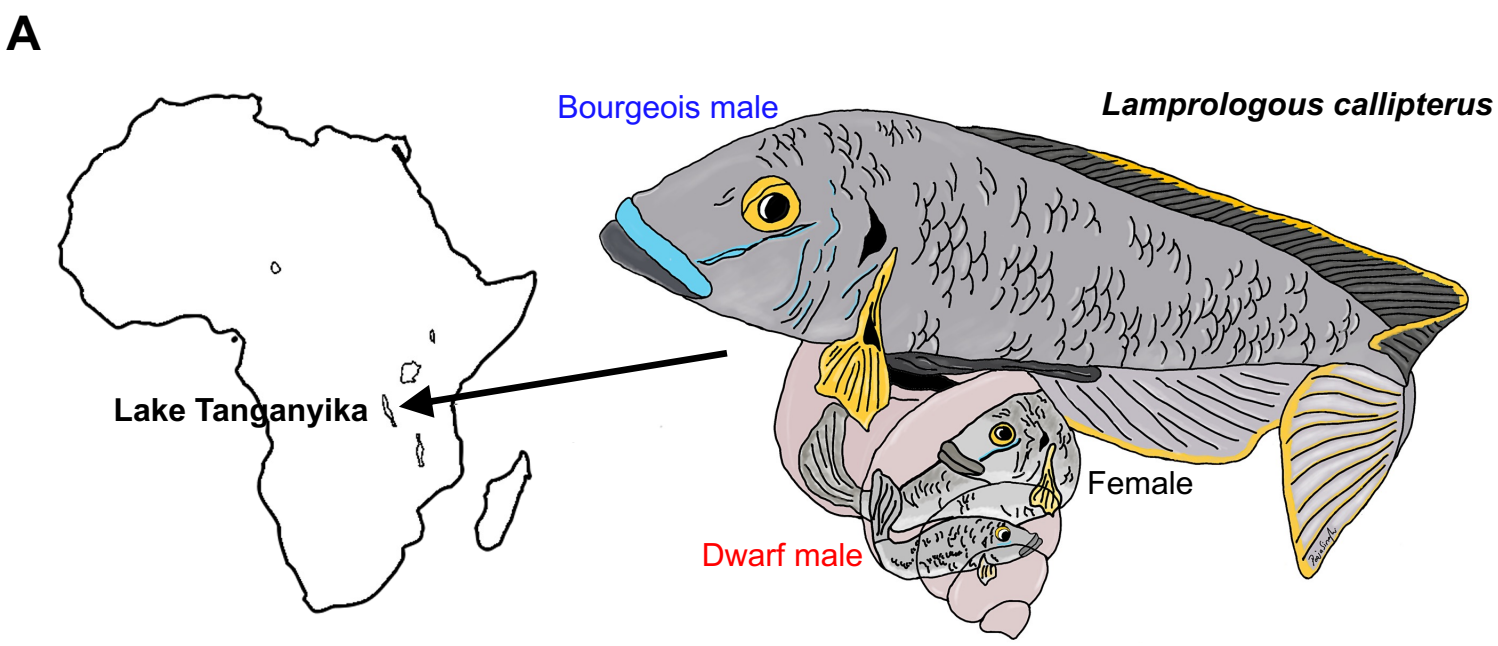

1365294x, ja, Downloaded from https://onlinelibrary.wiley.com/doi/10.1111/mec.16839 by Universität Be
rn, Wiley Online Library on [10/01/2023]. See the Terms and Conditions (https://onlinelibrary.wiley.com/terms-and-conditions)
on Wiley Online Library for rules of use; OA articles are governed by the applicable Creative Commons License

Figure 2

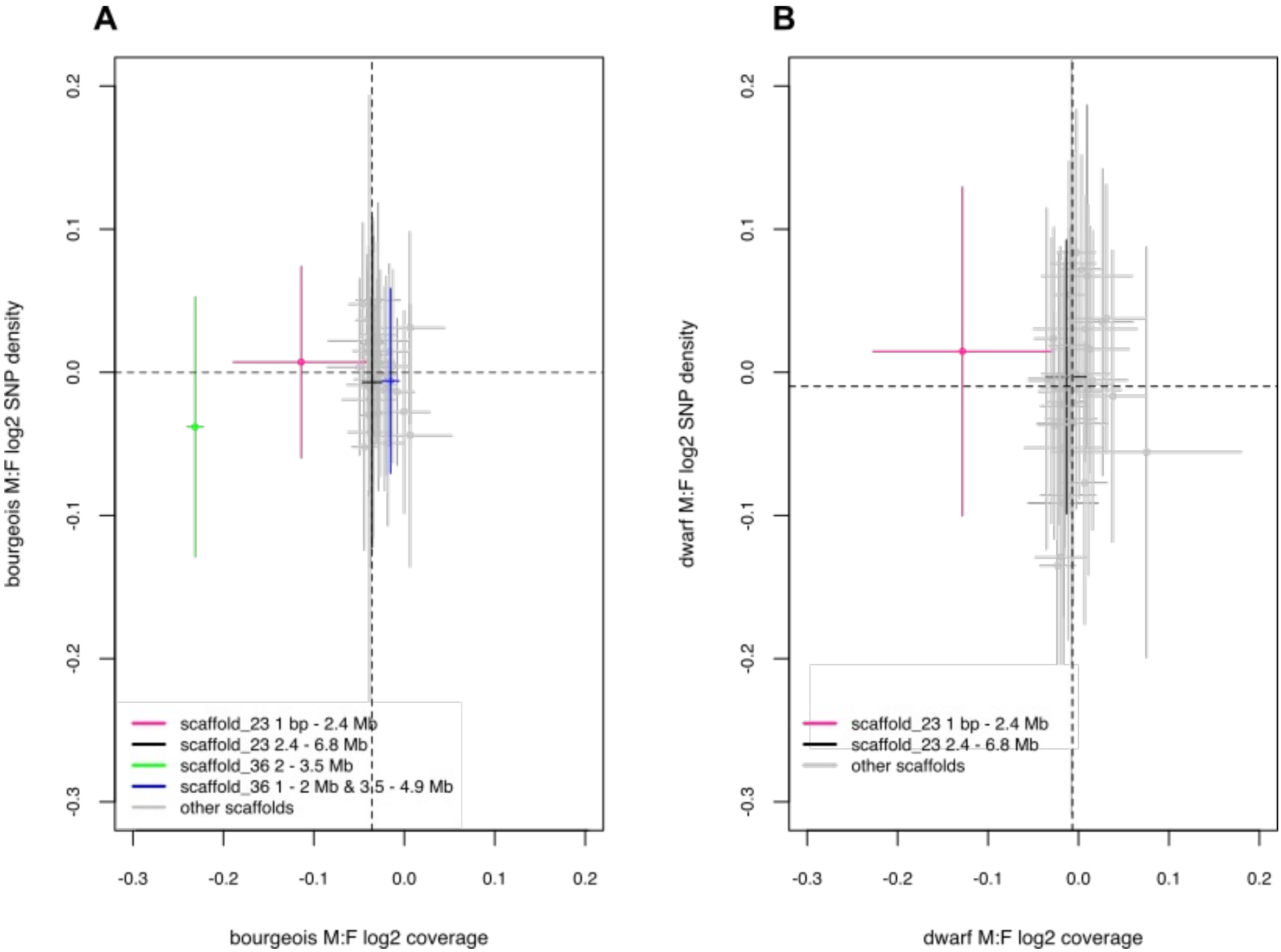

1365294x, ja, Downloaded from https://onlinelibrary.wiley.com/doi/10.1111/mec.16839 by Universität Bern, Wiley Online Library on [10/01/2023]. See the Terms and Conditions (https://onlinelibrary.wiley.com/terms-and-conditions) on Wiley Online Library for rules of use; OA articles are governed by the applicable Creative Commons License

Figure 3

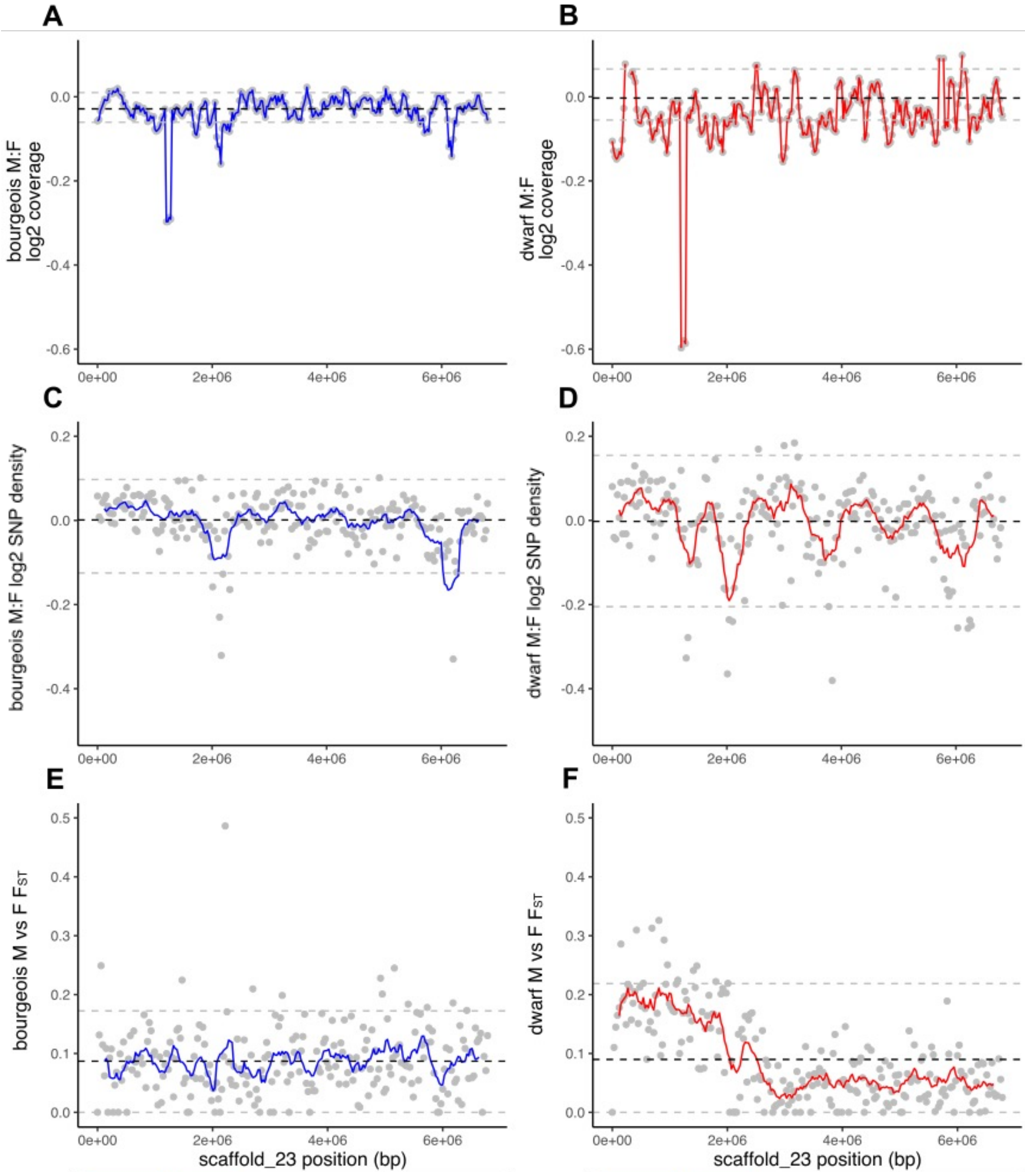

1365294x, ja, Downloaded from https://onlinelibrary.wiley.com/doi/10.1111/mec.16839 by Universität Bern, Wiley Online Library on [10/01/2023]. See the Terms and Conditions (https://onlinelibrary.wiley.com/terms-and-conditions) on Wiley Online Library for rules of use; OA articles are governed by the applicable Creative Commons License

Figure 4

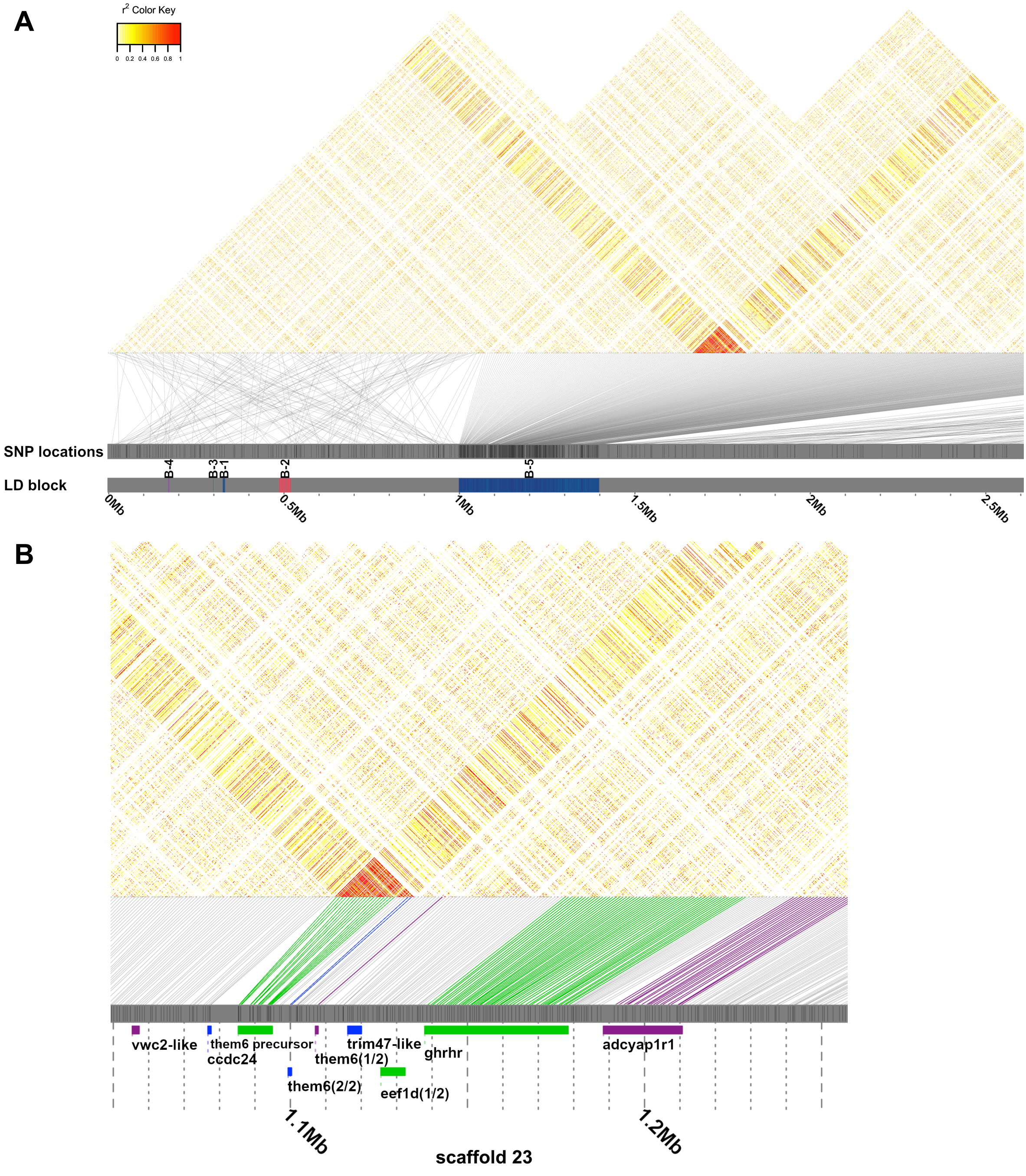

1365294x, ja, Downloaded from https://onlinelibrary.wiley.com/doi/10.1111/mec.16839 by Universität Bern, Wiley Online Library on [10/01/2023]. See the Terms and Conditions (https://onlinelibrary.wiley.com/terms-and-conditions) on Wiley Online Library for rules of use; OA articles are governed by the applicable Creative Commons License

Figure 5

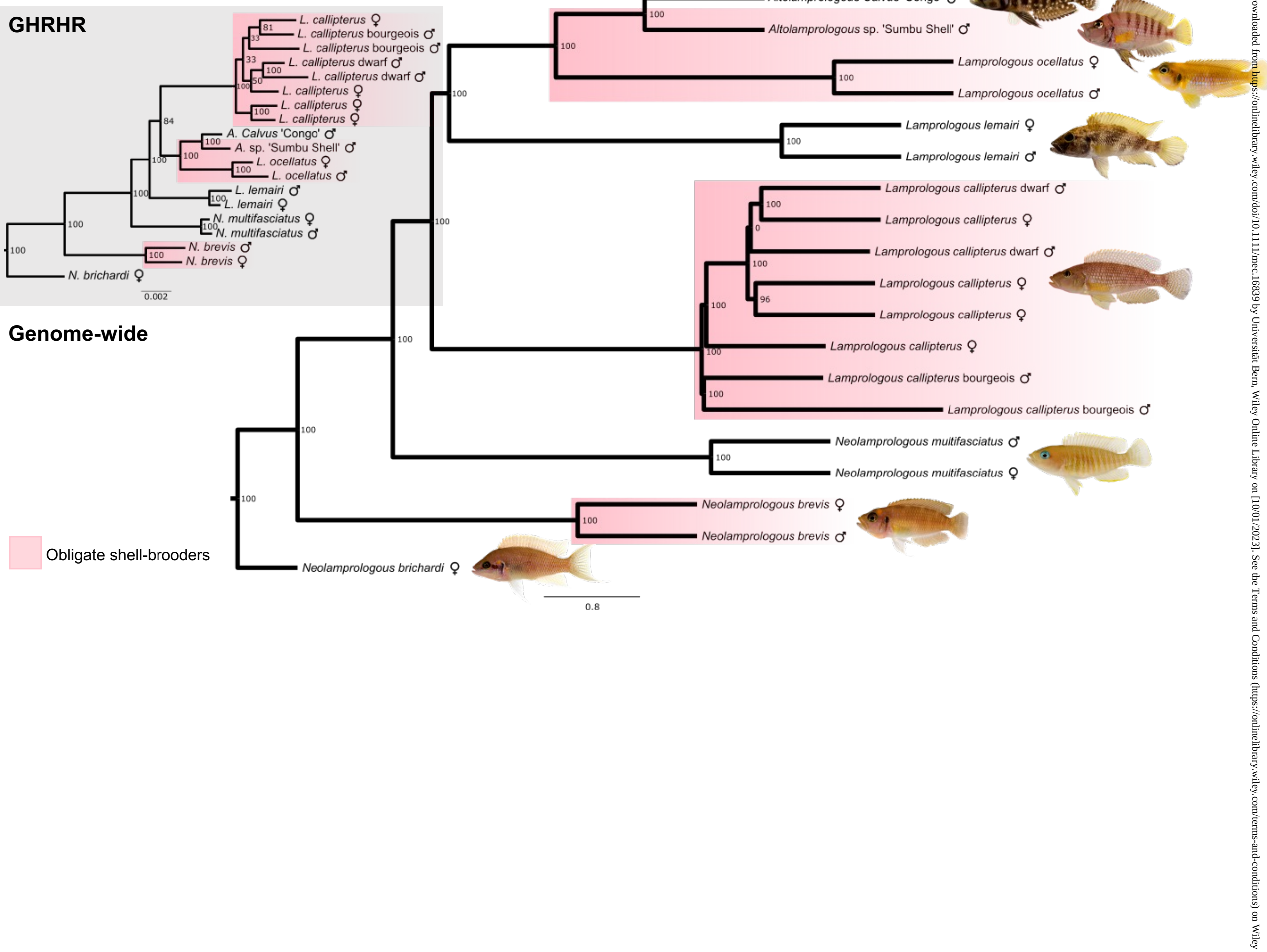

1365294x, ja, Downloaded from https://onlinelibrary.wiley.com/doi/10.1111/mec.16839 by Universität Bern, Wiley Online Library on [10/01/2023]. See the Terms and Conditions (https://onlinelibrary.wiley.com/terms-and-conditions) on Wiley Online Library for rules of use; OA articles are governed by the applicable Creative Commons License

Figure 6

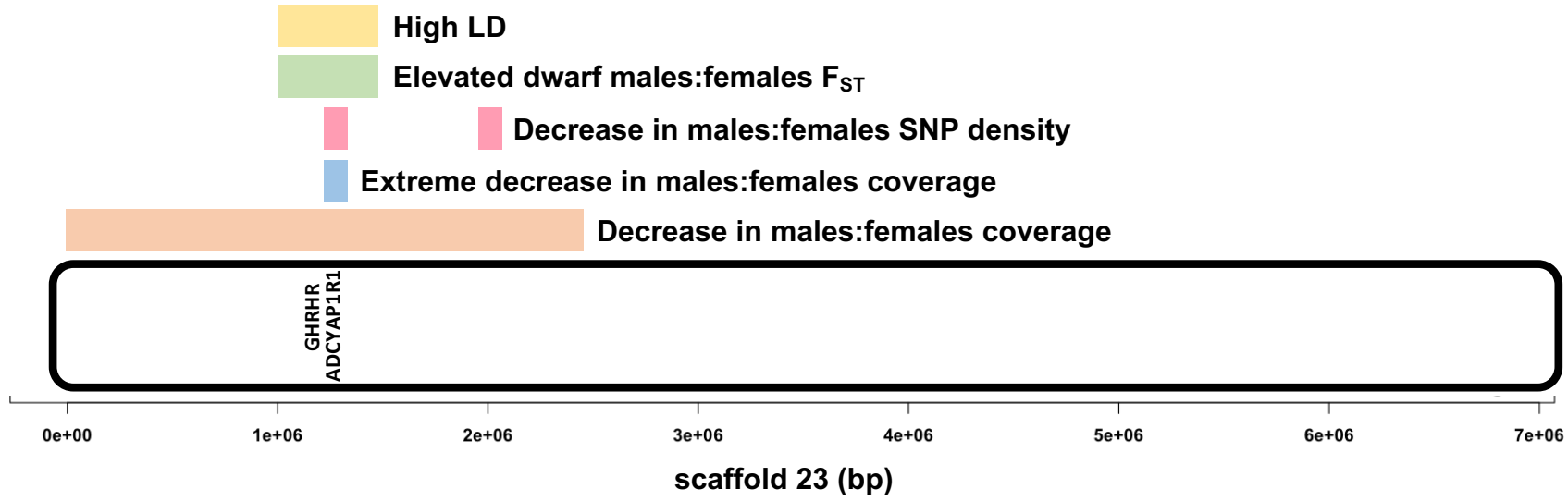

1365294x, ja, Downloaded from https://onlinelibrary.wiley.com/doi/10.1111/mec.16839 by Universität Bern, Wiley Online Library on [10/01/2023]. See the Terms and Conditions (https://onlinelibrary.wiley.com/terms-and-conditions) on Wiley Online Library for rules of use; OA articles are governed by the applicable Creative Commons License